Canada-France Ground Freezing Experiment: Phase VII

Spatial Variability of Heave Around a Pipeline and the Effects of Repeated Freezing and Thawing

Geotechnical Science Laboratories
Carleton University
Ottawa, Ontario
K1S 5B6

Report to Permafrost Section,
Terrain Sciences Division,
Geological Survey of Canada,
Energy, Mines and Resources Canada

July 1988

IR-55

FOREWORD

This report discusses certain findings from the third freeze cycle of the Canada-France pipeline ground freezing project as well as preliminary findings from the fourth cycle.

At the completion of the third freeze cycle it had become apparent that a number of improvements could be made to the instrumentation. Excavations were made for examination of the ground and instrumentation conditions. This was followed by installation of newly-constructed measuring equipment for examination of ground stress conditions.

The period reported on was unusual in other respects as well. In accordance with the wishes of the contracting agency the contract period was of only nine months duration such that this and future contract periods would terminate on March 30. Due to constraints on the funding available coupled with the wish to increase the proportion of funding allocated to the analysis of observations, the Canadian field project manager was withdrawn during the months of July and August, while a limited programme of readings was maintained by our French colleagues alone. Subsequently, on the return of the Canadian field project manager the preparatory work outlined was carried out with freezing commencing again in December 1987.

The resurgence of interest in Northern hydrocarbon development, with several major pipeline proposals again under consideration, has resulted in enquiries about the project and its findings from three major companies and three associated

latter about the 'unique data bank' and the essential importance of the findings of the project in relation to new design approaches. Negotiations have been initiated concerning the transfer of the findings to industry. Nevertheless, at the moment, Energy Mines and Resources, Canada, remains the sole direct financial source for the operation of the project by the Canadian side.

The essential role of our French colleagues is again acknowledged. The mathematical modelling procedures developed by Michel Fremond and his associates were the subject of a special seminar he gave, at Carleton University, with the help of his assistant Mme. Monique Levy. Representatives of industry and research organisations in Fairbanks, Alaska; Houston, Texas; Montreal; Toronto; and Ottawa attended.

This report was prepared by D.E. Patterson (Project Manager, Ottawa), Dr. M.W. Smith (Co-Principal Investigator) and Dr. P.J. Williams (Principal Investigator). Chapter 4 was written by M. Shen and B. Ladanyi from CINEP, Ecole Polytechnique de Montreal. The efforts of the Project Managers in France, members of the Centre du Geomorphologie, CNRS and Laboratoire Central des Ponts et Chaussees are greatly appreciated.

The Canada-France project is comprised of a team of Canadian and French scientists, graduate students and technicians. The project as a whole is supervised by a scientific committee. The members and their affiliations are listed below.

M. Jaime Aguirre-Puente, Laboratoire d'Aerothermique, Centre National de la Recherche Scientifique

M. J-P. Lautridou, Centre National de la Recherche Scientifique

* M. Michel Fremond, Laboratoire Central des Ponts et Chauss es

Dr. A. Judge, Earth Physics Branch, Energy, Mines and Resources, Canada

M. Chantereau, Laboratoire Central des Ponts et Chauss es

M.S. Philippe, Laboratoire Central des Ponts et Chauss es

Dr. M.W. Smith, Geotechnical Science Laboratories, Carleton University

** Dr. P.J. Williams, Geotechnical Science Laboratories, Carleton University

* chairman France
** chairman Canada

Table of Contents

1 Introduction 1
  1.1 General Comments 1
  1.2 Scope of this Report 1

2 Spatial Variability of Heave in the Silt Section during the Third Freeze 3
  2.1 General 3
  2.2 Spatial Variation of Frost Heave Around the Pipe . 4

3 Observations During the Fourth Freeze Cycle 7
  3.1 General conditions 7
  3.2 Soil heave and strain 7
  3.2 Soil temperatures at selected sites 17
  3.3 Pipe displacement 19
  3.4 Pipe stress 21
  3.5 Soil pressures from the Petur devices 23
  3.6 Soil pressures from Glotzl cells 25

4. A mathematical model for calculating stress and deformation fields in soils during freezing 27

References 33

1 Introduction

1.1 General Comments

As discussed in a previous report, instrumentation was refurbished between the third and fourth freeze cycles (Geotechnical Science Laboratories, 1988). The Petur cells (for measuring soil pressure) had to be repaired and were re-installed at several locations along the pipe axis in the silt section. One new site was added off the pipe axis in the silt. Each site (generally) has six Petur cells; four are designed to measure total pressure, while the remaining two are directional (measuring vertical and lateral components).

The magnet heave device was modified to correct certain electrical and mechanical problems.

Changes in the timing and frequency of observations were also made to facilitate data comparison from cycle to cycle.

1.2 Scope of this Report

This report examines the soil heave observations obtained during the third freeze cycle of this project in more detail. Particular attention is given to the changes in heave rate and temperature gradient over time. Since temperature gradients and heave were obtained at various points within the silt section, temporal and spatial variations in the heave characteristics can be examined.

Data for the first 145 days of the fourth freeze cycle is also presented and discussed in a preliminary manner. Detailed

comparison of these observations with those obtained during the third cycle will be the subject of a future report.

The timetable of events to date is shown in Table 1.1.

Table 1.1 Timetable of Events

Event	Date from	Date to	Operating Conditions Air/Ground temp. (C)	Operating Conditions Pipe temp. (C)
First Freeze	09/21/82	08/06/83	-0.75	-2.0
Surface Thaw	08/06/83	17/10/83	4.0	-2.0
Second Freeze	17/10/83	18/09/85	-0.75	-5.0
Second Thaw	18/09/85	01/02/86	4.0	ambient
Re-instru-mentation	01/02/86	03/03/86	-	-
Third Freeze	03/03/86	25/02/87	-0.75	-5.25
Third Thaw	25/02/87	21/05/87	4.0	ambient
Shutdown	21/05/87	06/01/88	-	-
Fourth Freeze	06/01/88	-	-0.75	-5.25

2 Spatial Variability of Heave in the Silt Section during the Third Freeze

2.1 General

A significant observation from the third freeze cycle was that frost heave does not originate solely at a single, "primary" active ice lens in the soil but that vertical displacement of the soil involves continuing internal deformation of the frozen soil itself. Thus a considerable thickness of soil may be significantly affected by moisture movement and ice accumulation during frost heaving. As such, the nature of frost heaving is distinctly different to that visualised in the current (one-dimensional) models of the process.

These observations raise important conceptual issues in the understanding of the frost heave process. It is suggested that frost heave occurs at a rate which depends in a complex manner on the thermodynamic conditions of temperature and water and ice pressures as they are modified by the creep properties (rheology) of the soil. Substantially greater heaving pressures results from ice growth at low temperatures, which should be of significance to geocryologic processes and engineering. These aspects are discussed in more detail in Smith and Patterson (submitted for publication) and Geotechnical Science Laboratories (1988). Preliminary analysis of results from the fourth freeze cycle confirm this behaviour

2.2 Spatial Variation of Frost Heave Around the Pipe

The total heave at any location is obviously influenced by the proximity of the cold pipe but it is also affected by the mechanical constraint that the pipe imposes on the soil. For, within the silt, the pipe (and hence the surrounding soil) is restrained from heaving freely by virtue of the fact that one half of it is "anchored" in the sand. In order to examine this effect, we standardised the heave data with respect to the temperature conditions following the method of Konrad and Morgenstern (1981).

They describe the frost heaving behaviour of a silty soil in terms of a segregation potential, defined as the ratio of:

$$SP = \frac{H}{1.09 \text{ grad } T} \quad mm^2 \, s^{-1} \, C^{-1} \qquad (1)$$

where H is the heave rate and grad T is the temperature gradient at the frost line. Konrad and Morgenstern (1981) also described the effect of overburden pressure on this parameter.

The ratio in equation (1) was calculated throughout the period 100 to 300 days of the third freeze cycle; prior to 100 days, the highly transient nature of the freezing process renders this approach unsuitable. The analysis included sites 1, 2, 6 and 7 along the pipe axis, and sites 3 and 4 along the BB cross-section normal to the pipe. The "segregation potential" values calculated for these sites are shown in Figure 2.1. This figure reveals the variable manner in which the mechanical interaction between the pipe and the soil affects the frost heave.

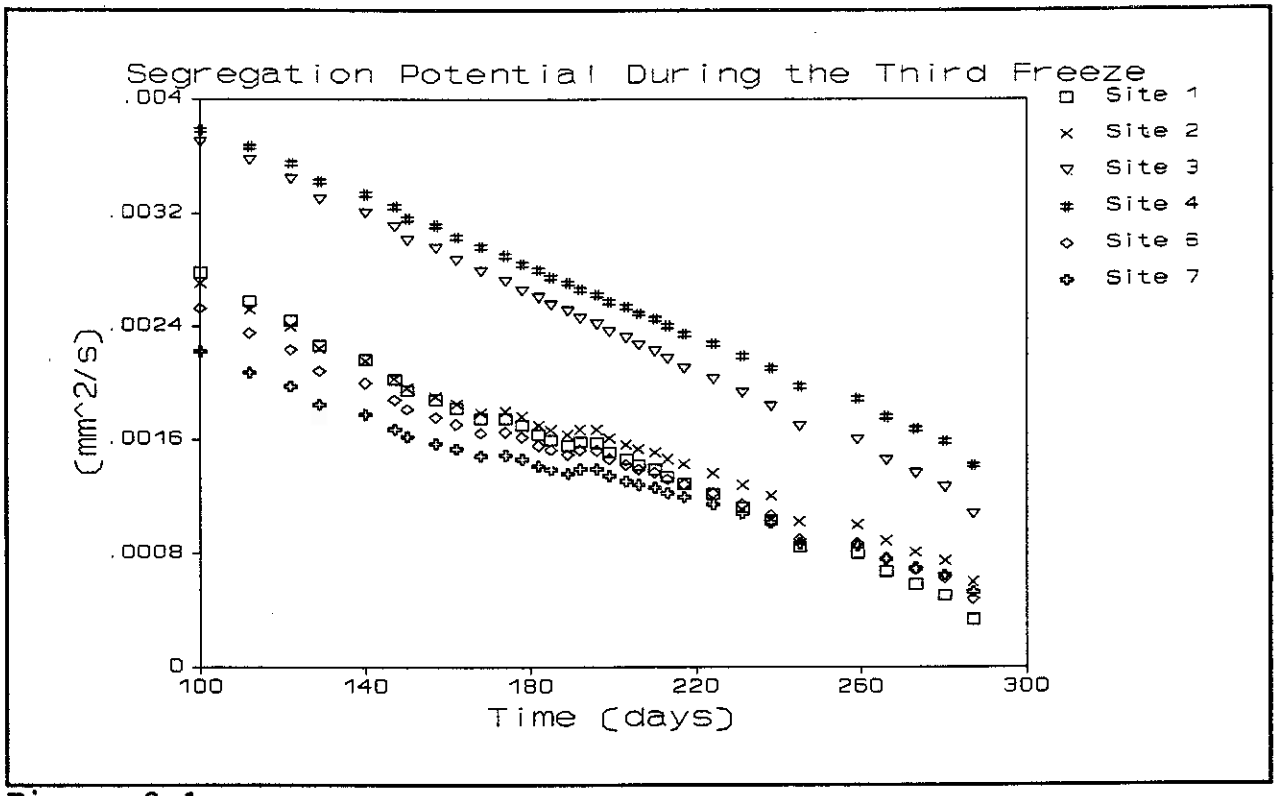
Segregation Potential During the Third Freeze
Site 1
Site 2
Site 3
Site 4
Site 6
Site 7
(mm^2/s)
.004
.0032
.0024
.0016
.0008
0
100
140
180
220
260
300
Time (days)

Figure 2.1

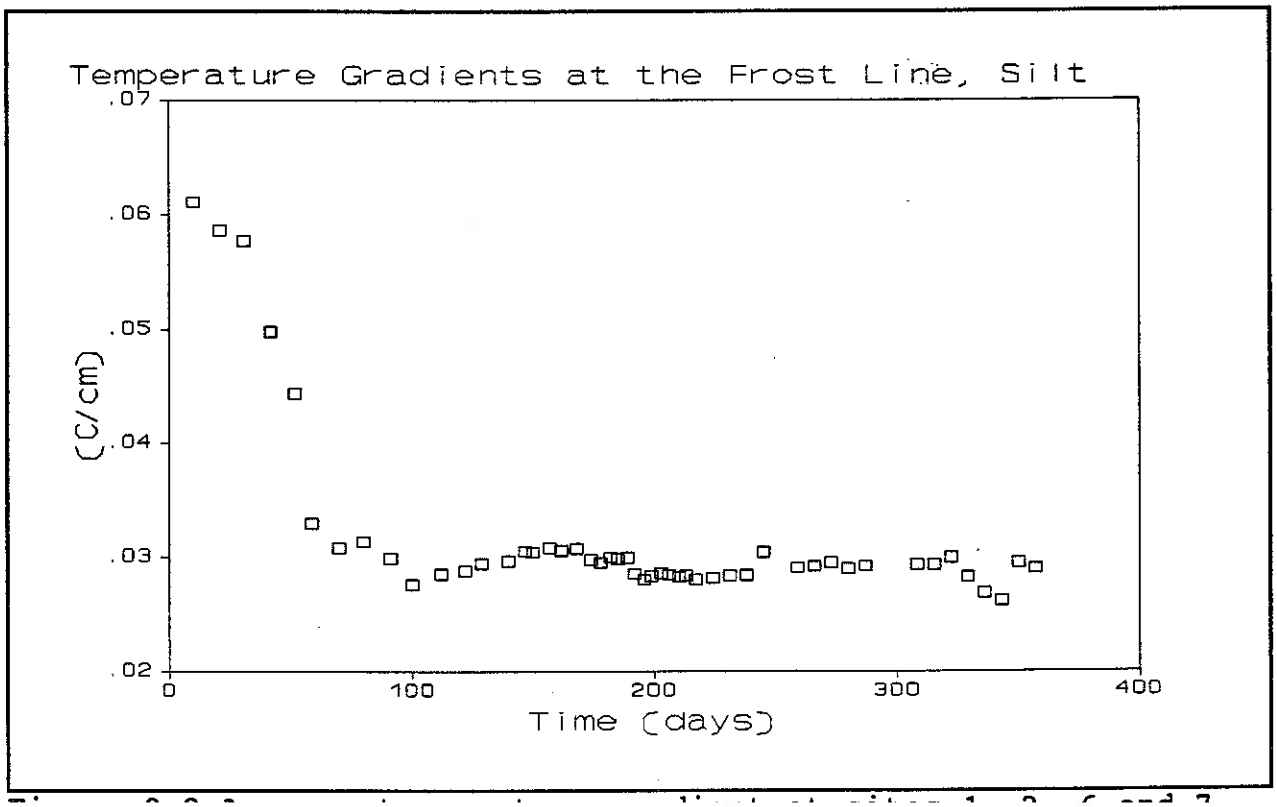
Temperature Gradients at the Frost Line, Silt
(C/cm)
.07
.06
.05
.04
.03
.02
0
100
200
300
400
Time (days)

At all the sites the ratio decreases with time, even though the temperature gradient at each remains essentially constant throughout the period (e.g. Figure 2.2). This decrease can be explained by the increasing restraint imposed upon the freezing soil by the pipeline-frozen soil annulus system. The sites off the pipe axis show higher values than those located along the axis, as a result of the reduced influence of the pipe-soil annulus. The further away from the pipe (site 4), the less restrained the frost heaving is. Similarly, as one proceeds along the pipe towards the silt-sand transition, the frost heave is increasingly restrained. Figure 2.1 illustrates that such simplistic notions as the segregation potential are unable to describe the real complexity of frost heaving around a pipeline. The interaction between the pipe and the freezing soil introduces three-dimensional, time-dependent effects which cannot be easily prescribed a priori but evolve as an integral part of the problem.

3 Observations During the Fourth Freeze Cycle

3.1 General conditions

The temperature conditions for this freeze cycle are the same as those used during the second and third cycles. The compressors controlling air and pipe temperature are still maintained at approximately -0.75 and -5.25 C respectively. The water table is maintained at 90 cm beneath the soil surface, as in the past.

3.2 Soil heave and strain

Figures 3.1 to 3.12 show total heave and differential strain for selected sites during the first 145 days of the fourth freeze cycle. The patterns emerging are similar to those noted during the third freeze cycle. For the sites along the pipe axis, heave tends to decrease the closer the site is to the sand-silt transition (sites 1, 2, 6, 7). As in the previous cycle, heave decreases the further the site is from the pipe axis (sites 2, 3 and 4).

The depth ranges indicated on the differential strain figures refer to the initial magnet position prior to freeze (to the nearest cm). The strain patterns for all sites show a high heave rate with a lower total strain in the early periods of the freeze followed by lower heave rates and greater total strain as freezing progresses. This was noted in the previous cycle. As the progression of the freezing front slows, and the temperature gradients become smaller, water movement and ice accumulation will be greater per unit volume.

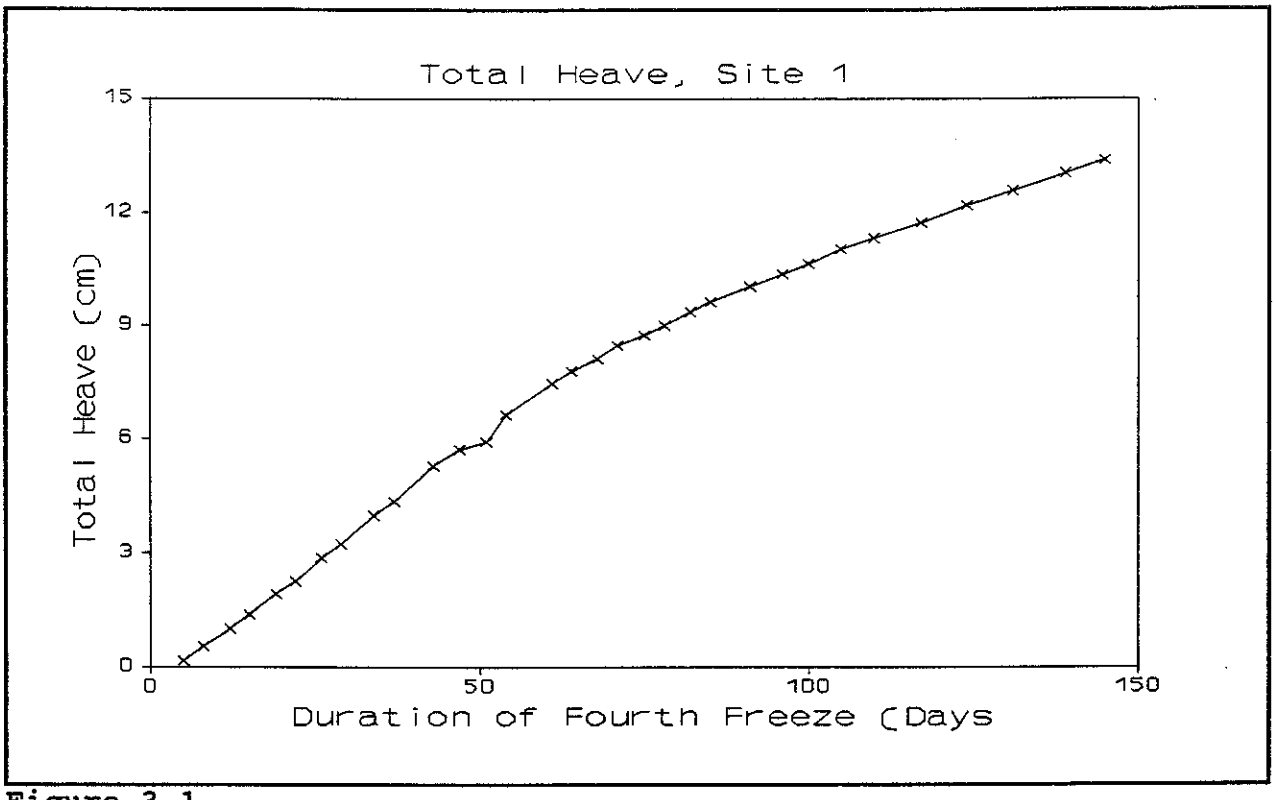
Total Heave, Site 1
Total Heave (cm)
0
3
6
9
12
15
0
50
100
150
Duration of Fourth Freeze (Days

Figure 3.1

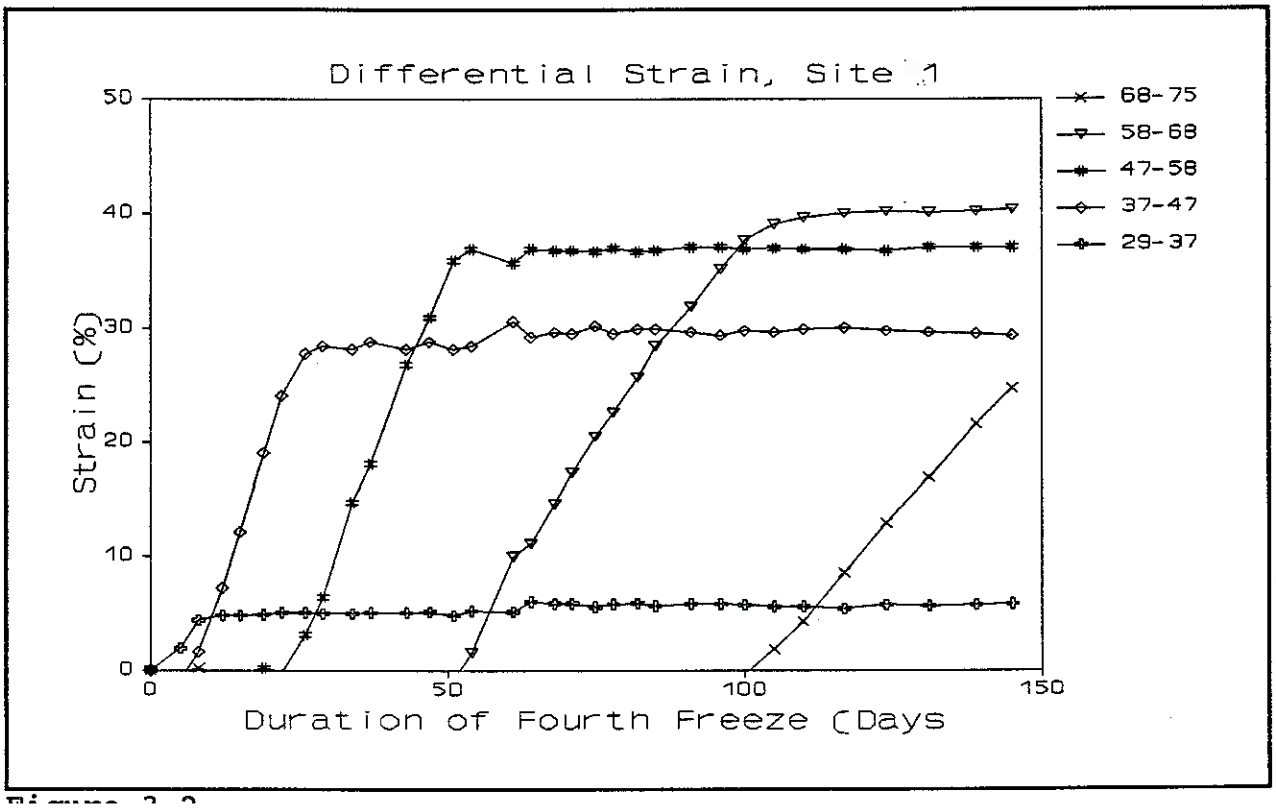
Differential Strain, Site 1
Strain (%)
0
10
20
30
40
50
0
50
100
150
Duration of Fourth Freeze (Days
68-75
58-68
47-58
37-47
29-37

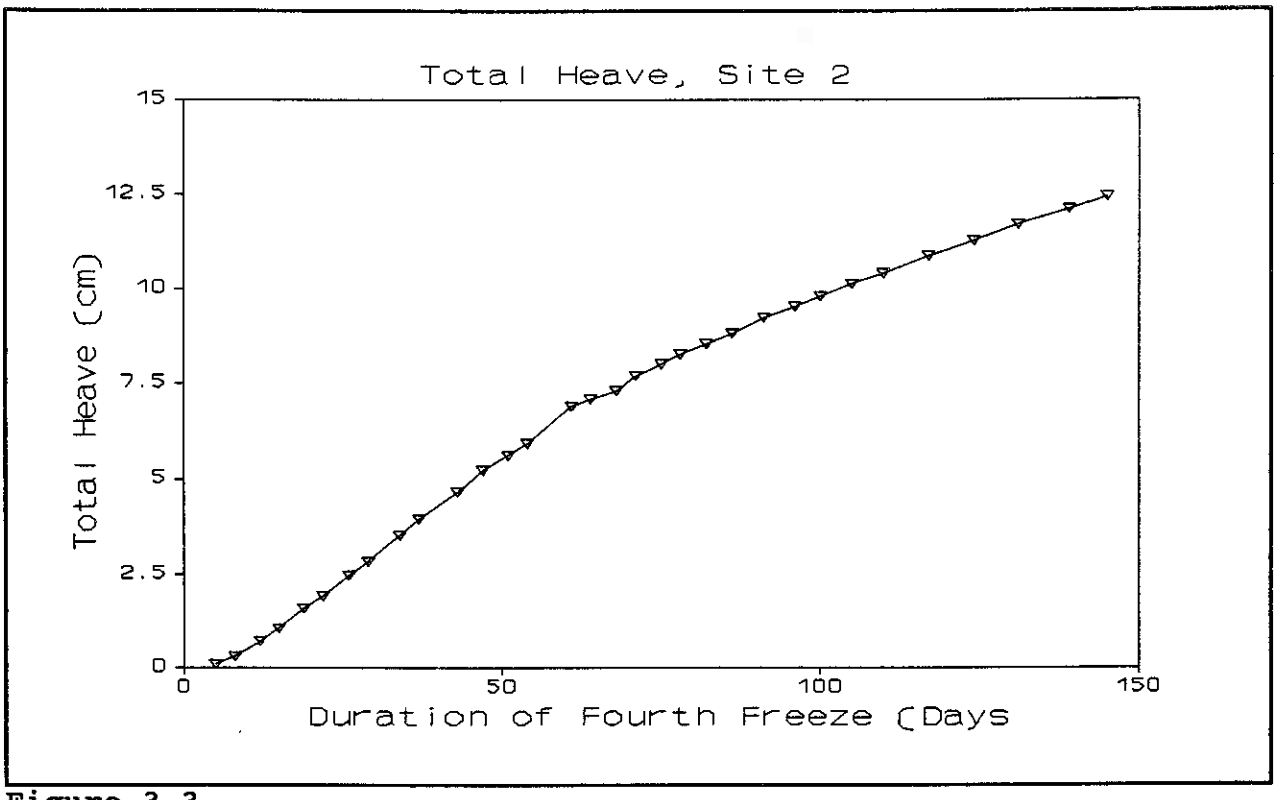
Total Heave, Site 2
Total Heave (cm)
15
12.5
10
7.5
5
2.5
0
0
50
100
150
Duration of Fourth Freeze (Days

Figure 3.3

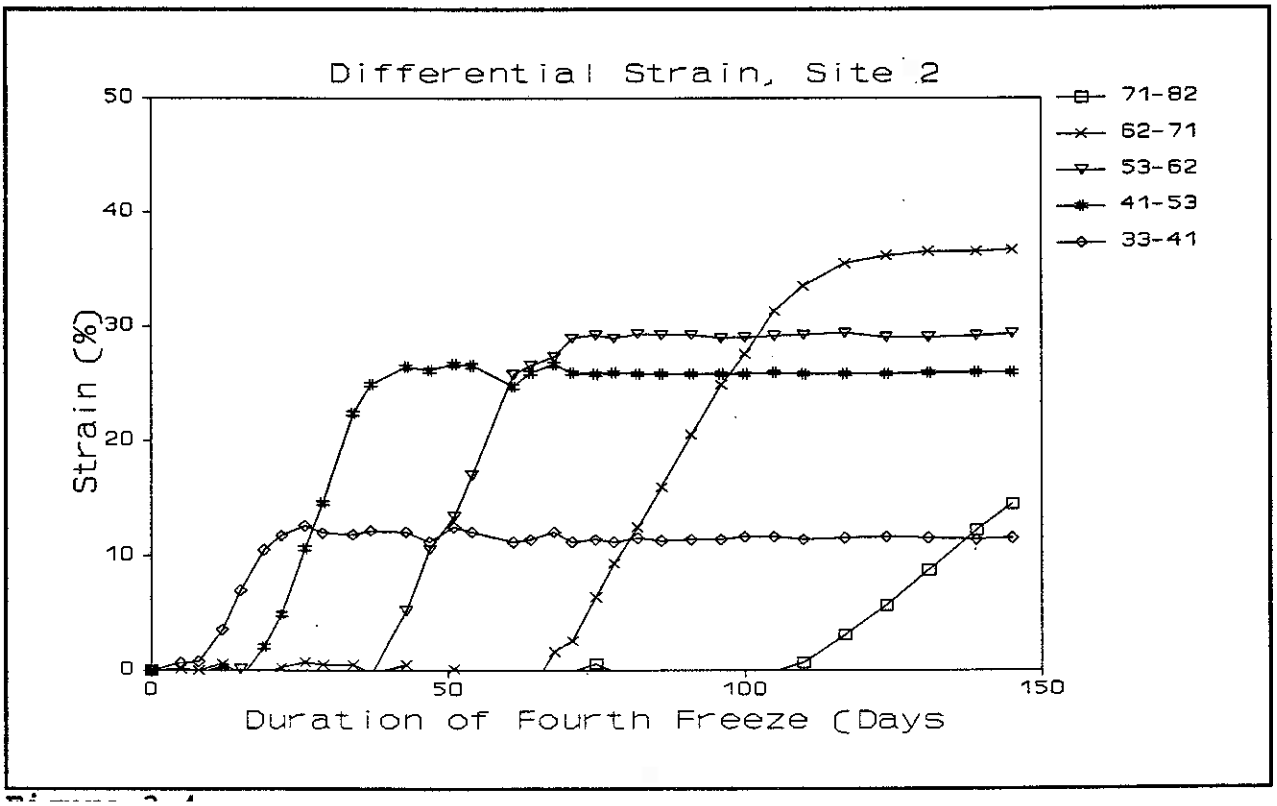
Differential Strain, Site 2
Strain (%)
50
40
30
20
10
0
0
50
100
150
Duration of Fourth Freeze (Days
71-82
62-71
53-62
41-53
33-41

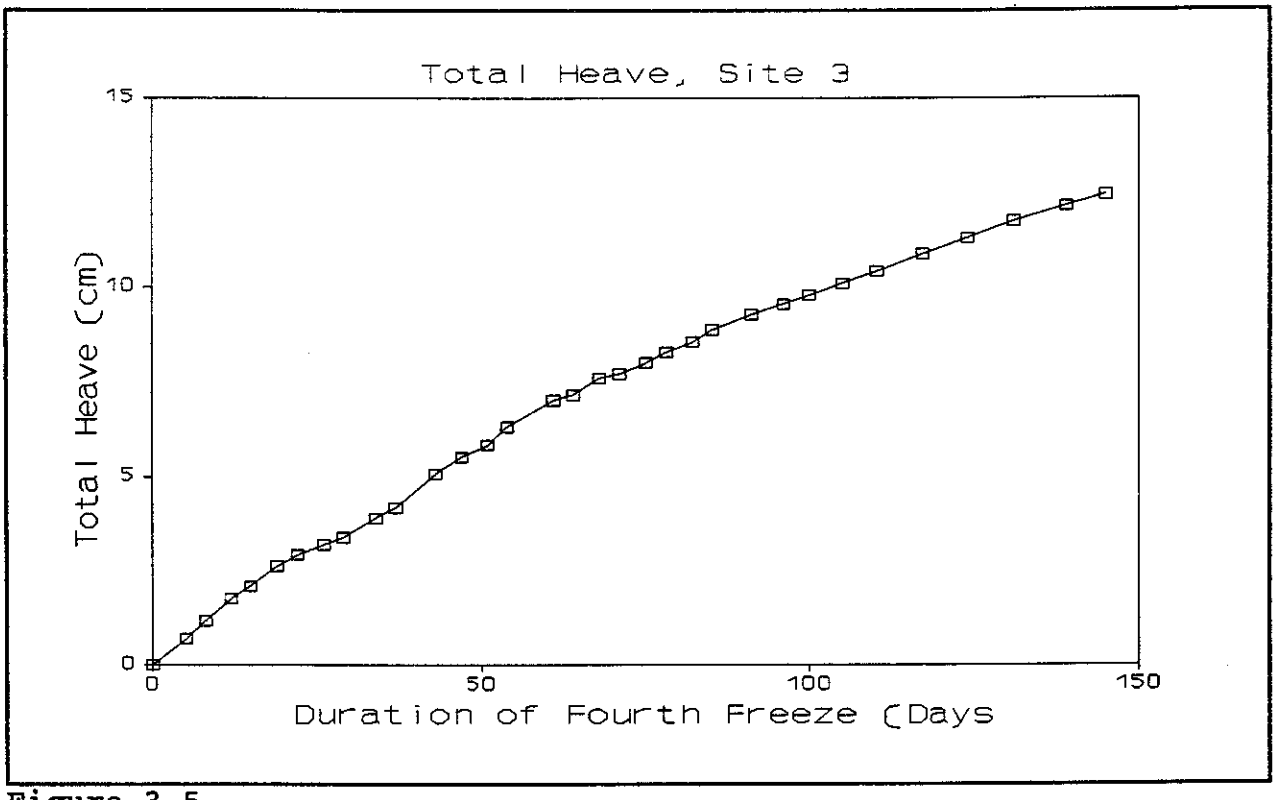
Total Heave, Site 3
Total Heave (cm)
Duration of Fourth Freeze (Days
0
5
10
15
0
50
100
150

Figure 3.5

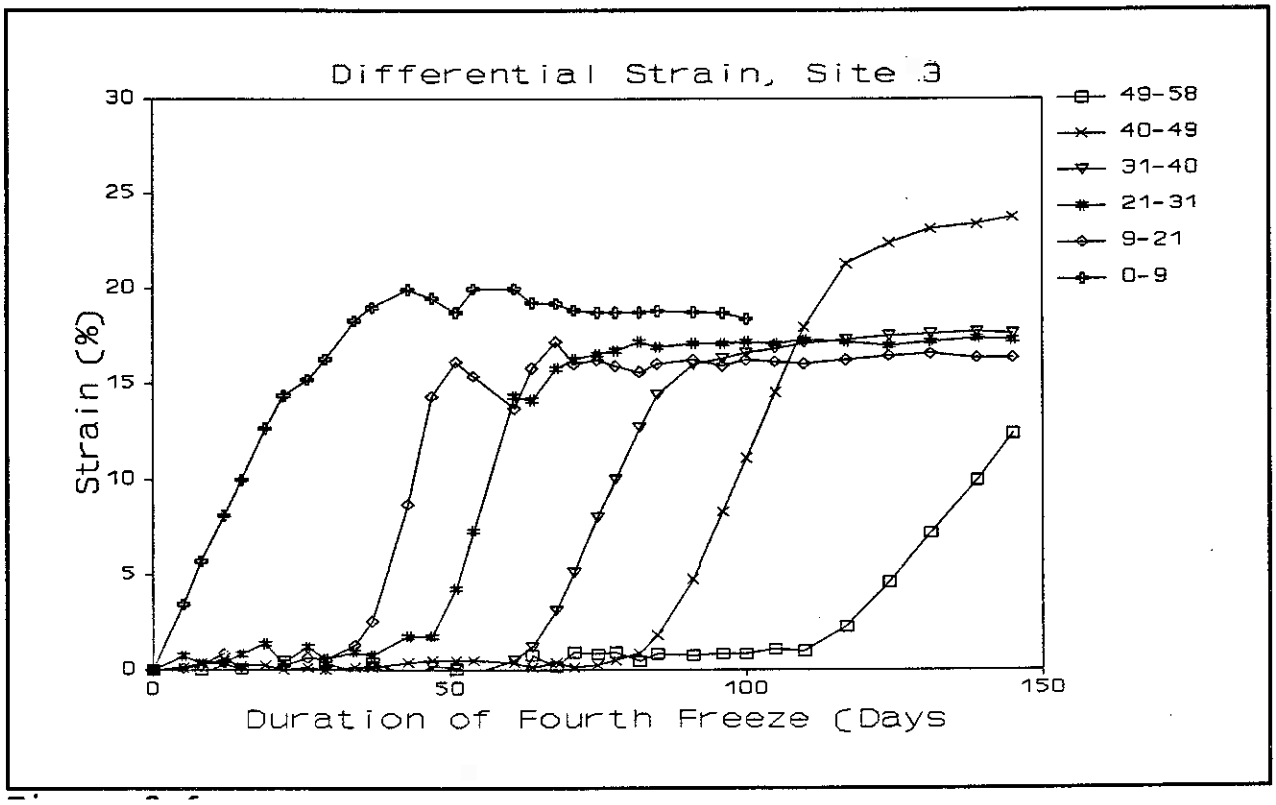
Differential Strain, Site 3
Strain (%)
Duration of Fourth Freeze (Days
0
5
10
15
20
25
30
0
50
100
150
49-58
40-49
31-40
21-31
9-21
0-9

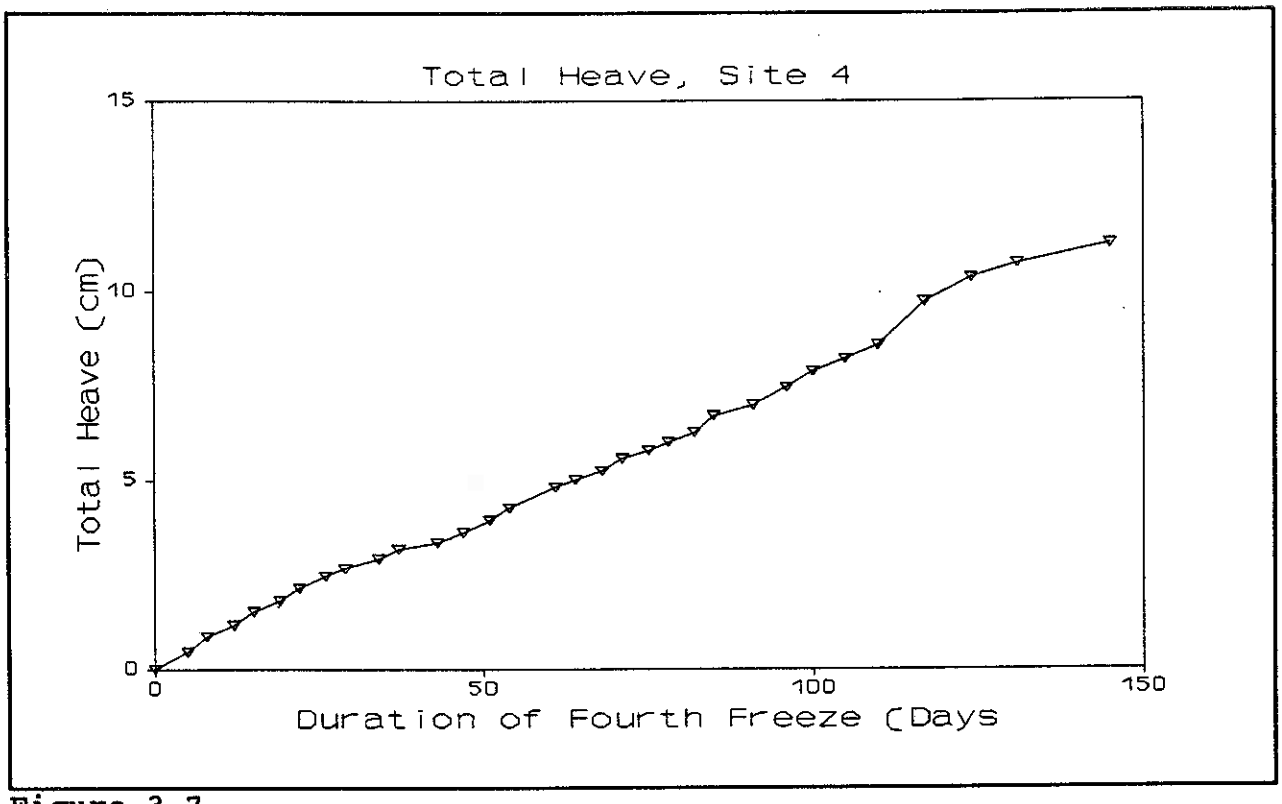
Total Heave, Site 4
Total Heave (cm)
0
5
10
15
0
50
100
150
Duration of Fourth Freeze (Days

Figure 3.7

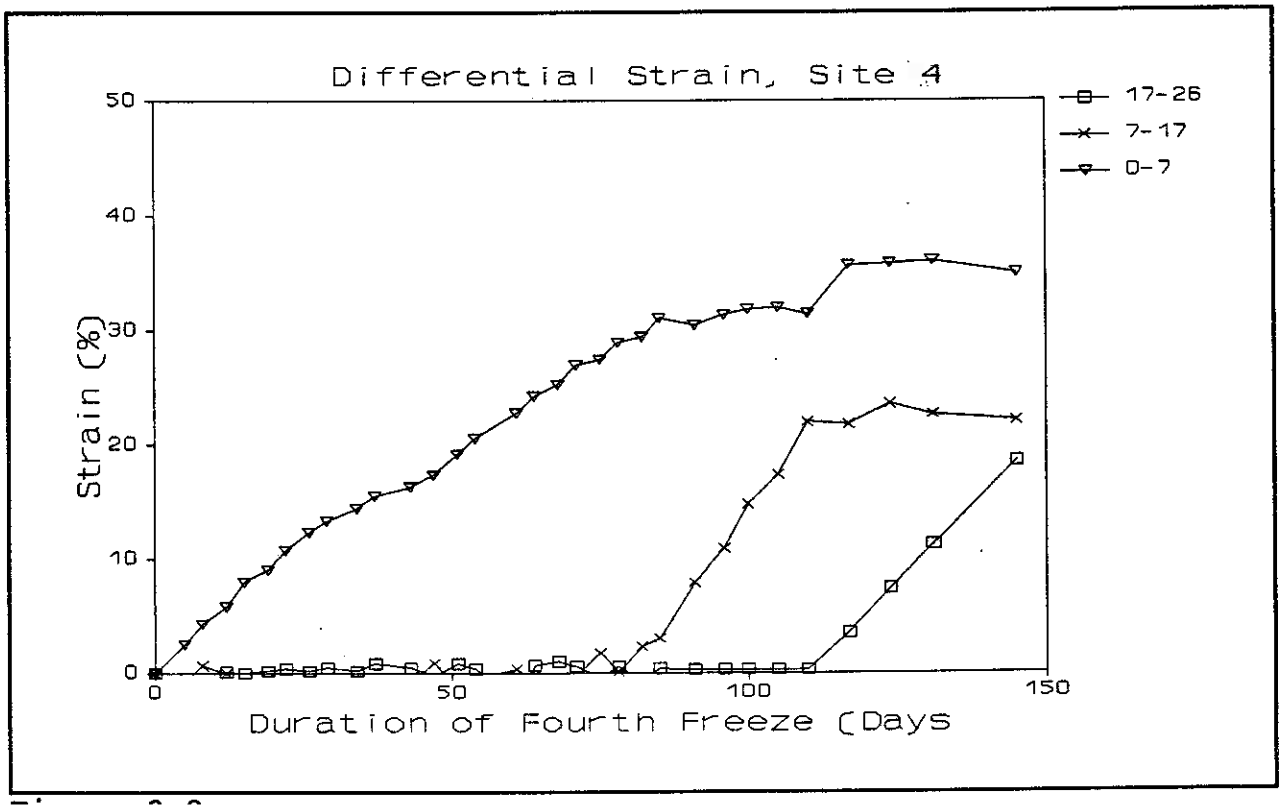
Differential Strain, Site 4
17-26
7-17
0-7
Strain (%)
0
10
20
30
40
50
0
50
100
150
Duration of Fourth Freeze (Days

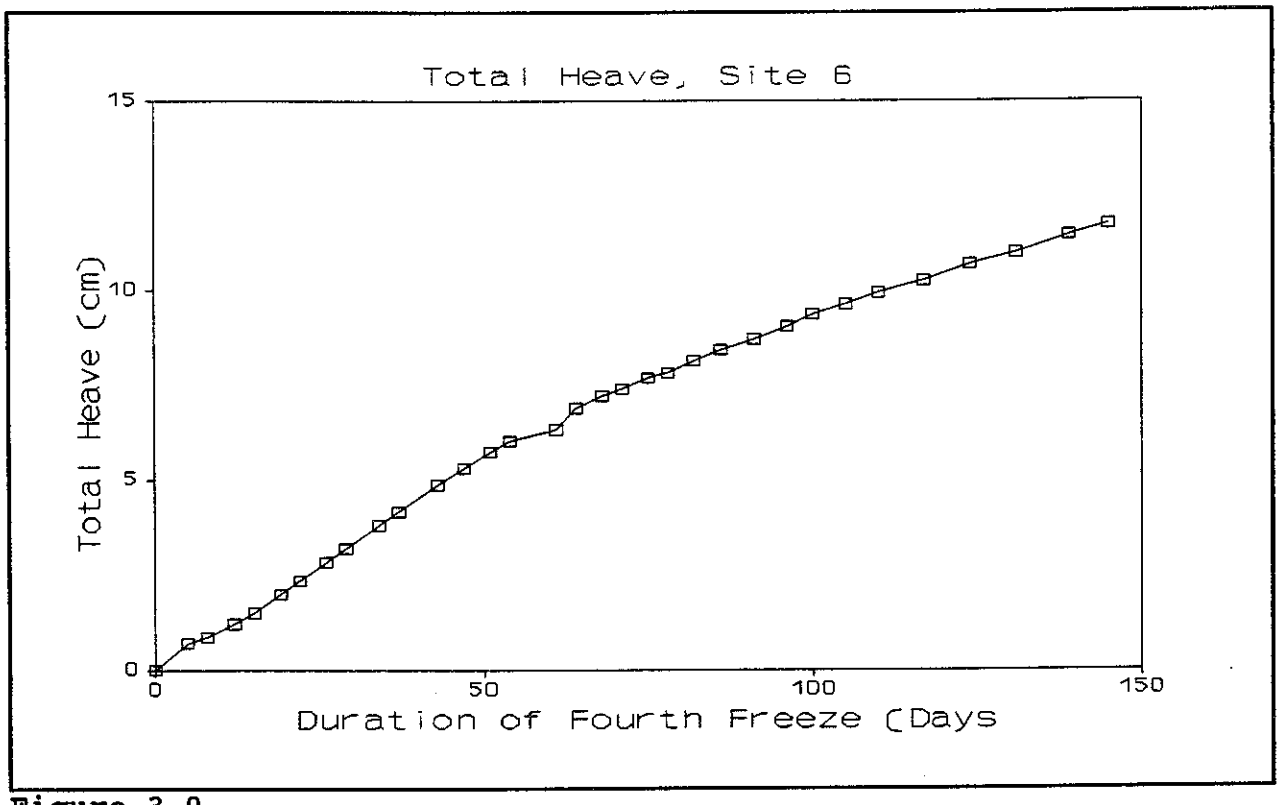
Total Heave, Site 6
Total Heave (cm)
0
5
10
15
0
50
100
150
Duration of Fourth Freeze (Days

Figure 3.9

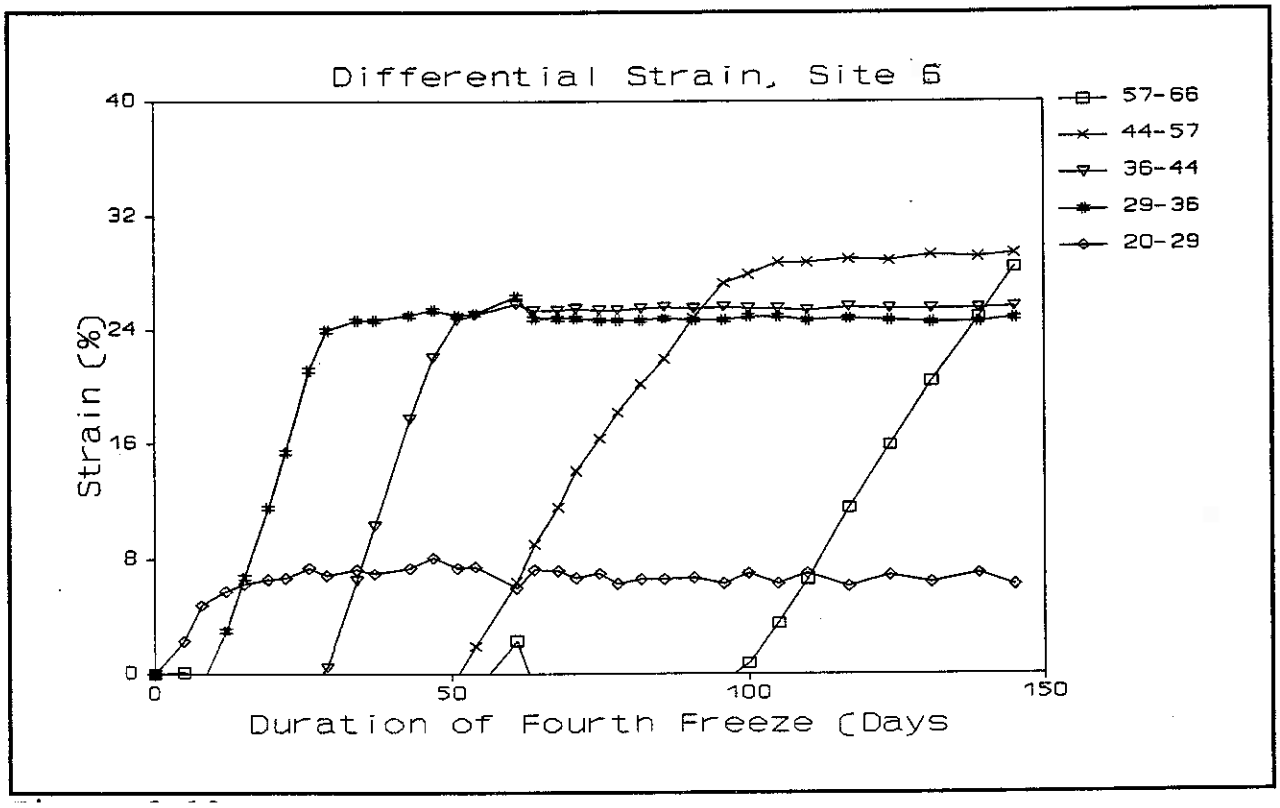
Differential Strain, Site 6
Strain (%)
0
8
16
24
32
40
0
50
100
150
Duration of Fourth Freeze (Days
57-66
44-57
36-44
29-36
20-29

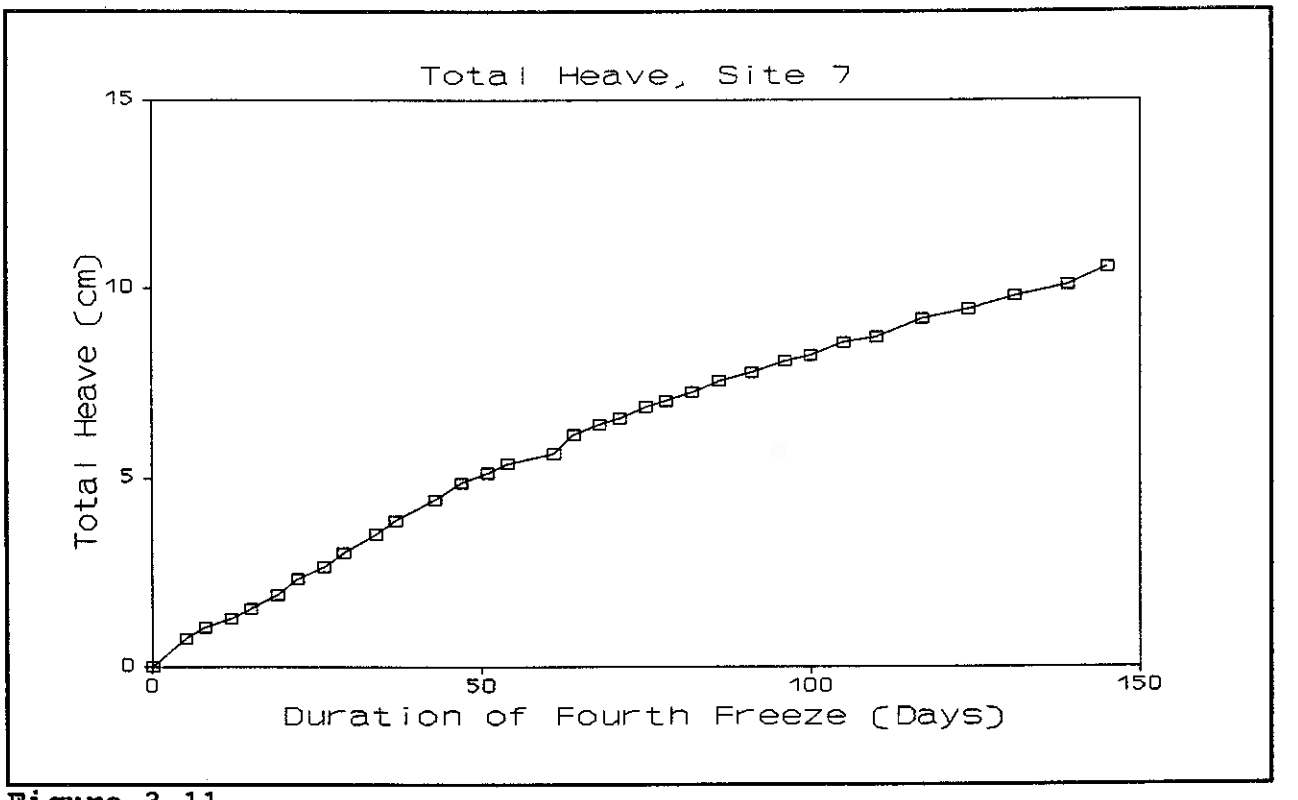
Total Heave, Site 7
Total Heave (cm)
0
5
10
15
0
50
100
150
Duration of Fourth Freeze (Days)

Figure 3.11

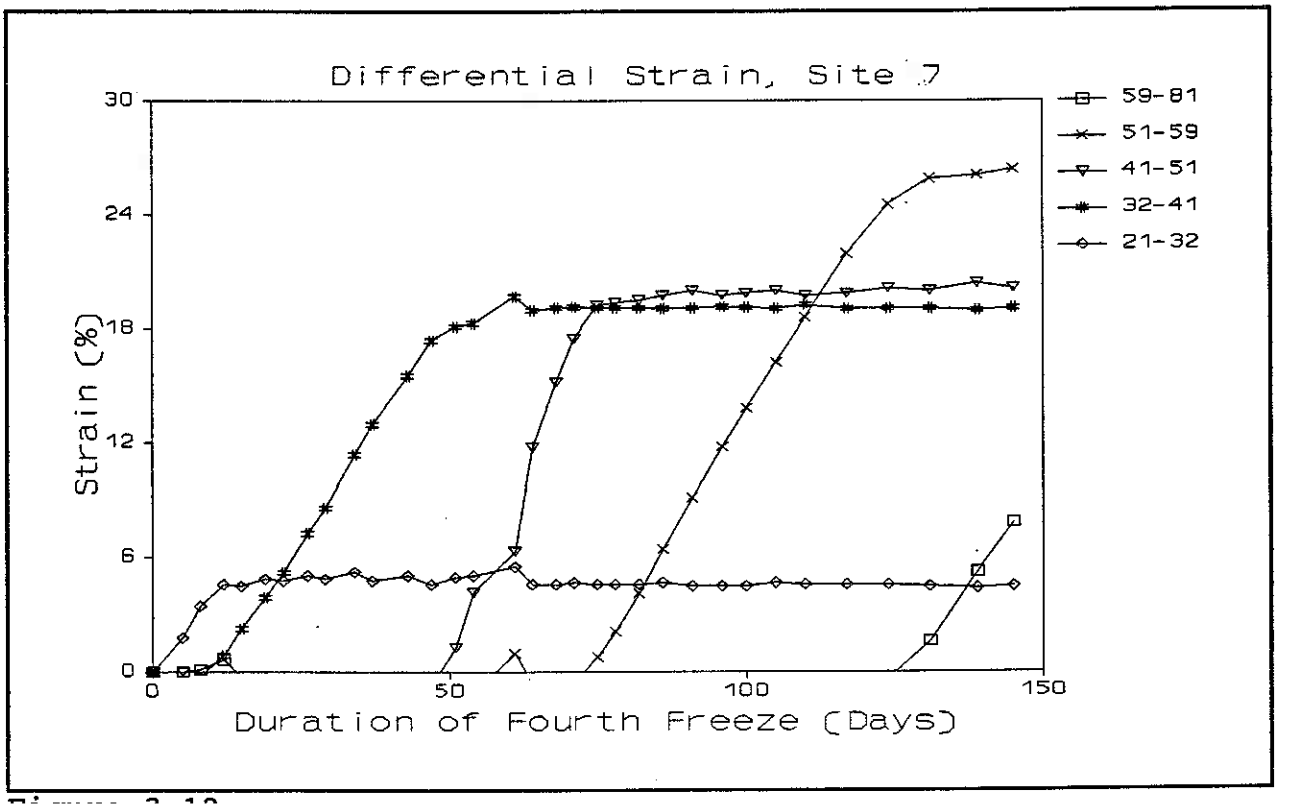
Differential Strain, Site 7
Strain (%)
0
6
12
18
24
30
0
50
100
150
Duration of Fourth Freeze (Days)
59-81
51-59
41-51
32-41
21-32

The amount of strain occuring in already frozen ground in the early period of the freeze cycle is quite small for all sites. At site 2 (Figures 3.4), continuing strain is evident in the 62-71 cm layer after day 108. Similarly, the 40-49 cm layer at site 3 (Figure 3.6) is showing evidence of continuing strain.

The amount of continuing strain will be greatest, the smaller the temperature gradient and the slower the rate of frost penetration. At this early stage of the cycle, the freezing rates are beginning to decrease and subsequent observations should substantiate the observations made earlier (Geotechnical Science Laboratories, 1988).

Figures 3.13 and 3.14 present a comparison of heave for sites 2 and 4 respectively for the first 150 days of the third and fourth freeze cycle. Site 2 is located in the silt section near the BB transition about 25 cm off the pipeline axis. Site 4 is located about 1 m from the pipeline axis in line with site 2. The heave at site 2 is similar between these freeze cycles while site 4 shows marked differences. It is premature to speculate as to possible reasons until more information is obtained.

Figures 3.15 and 3.16 show heave rates for sites 2 and 4, respectively, during the fourth freeze cycle. The heave rate for site 2 was higher during the first 50 days, decreasing thereafter. The heave rate for site 4 is variable but shows no trend. These aspects will be examined further.

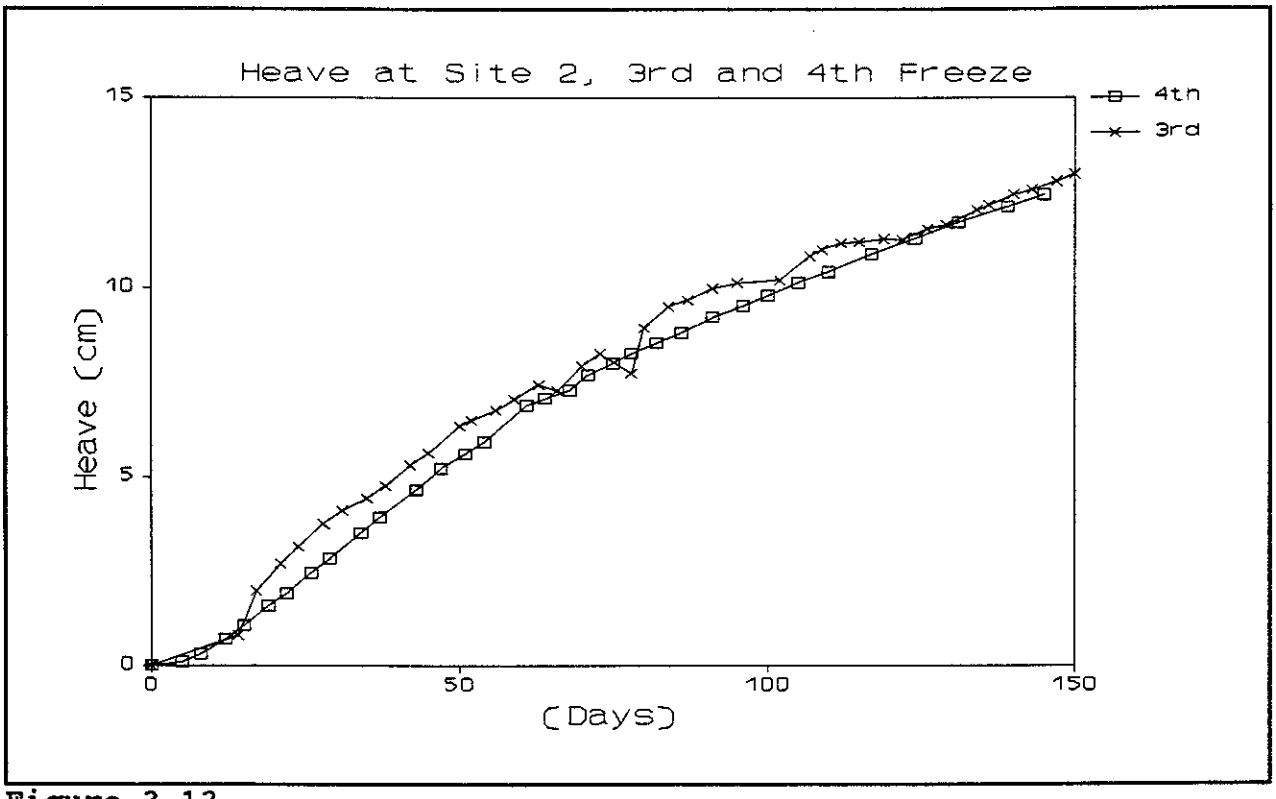
Heave at Site 2, 3rd and 4th Freeze
4th
3rd
Heave (cm)
(Days)
0
5
10
15
0
50
100
150

Figure 3.13

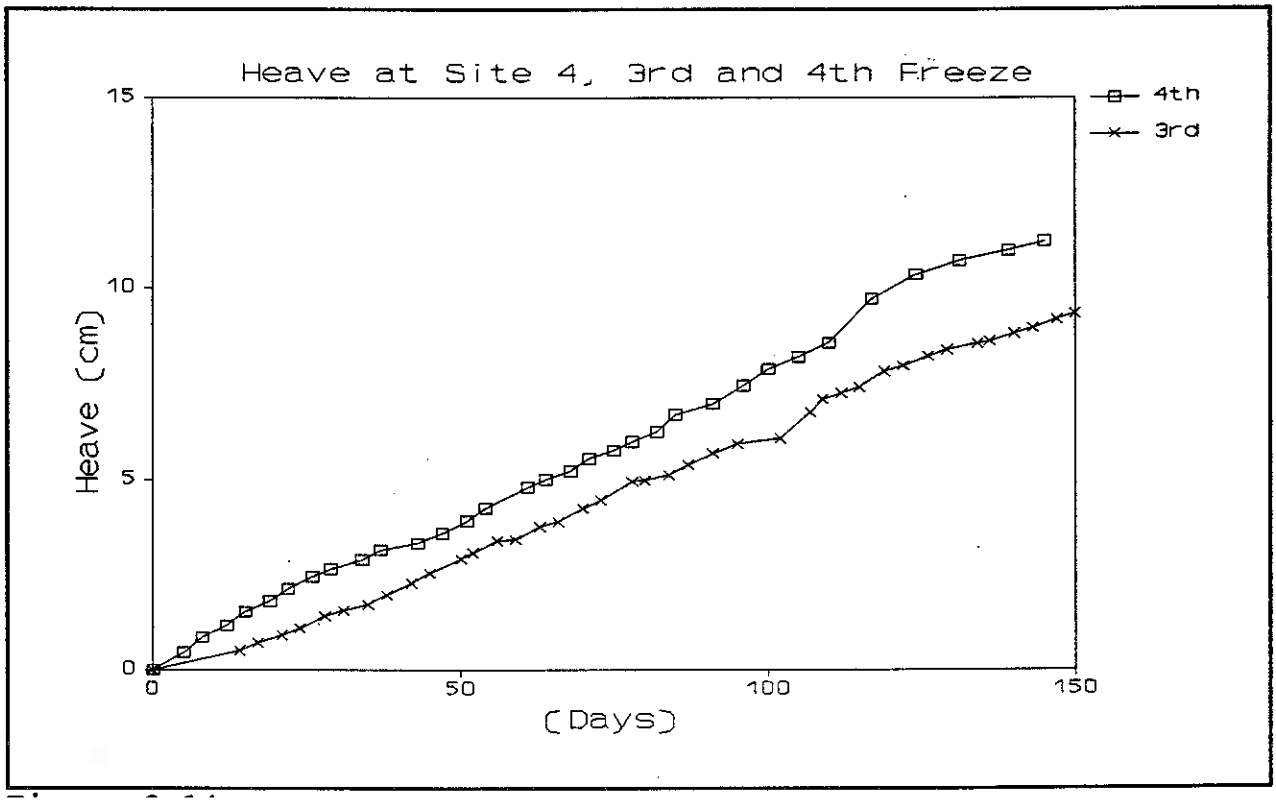
Heave at Site 4, 3rd and 4th Freeze
4th
3rd
Heave (cm)
(Days)
0
5
10
15
0
50
100
150

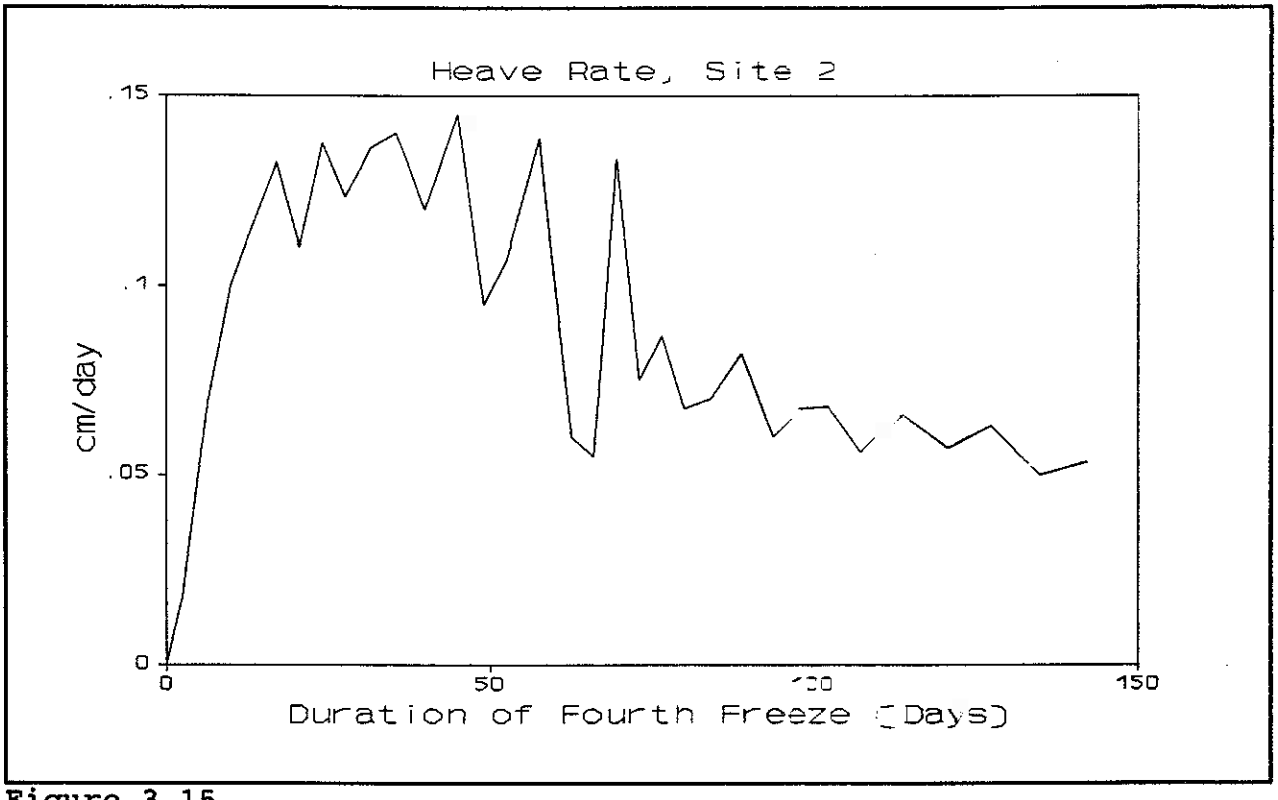
Heave Rate, Site 2
.15
.1
.05
0
cm/day
0
50
150
Duration of Fourth Freeze [Days]

Figure 3.15

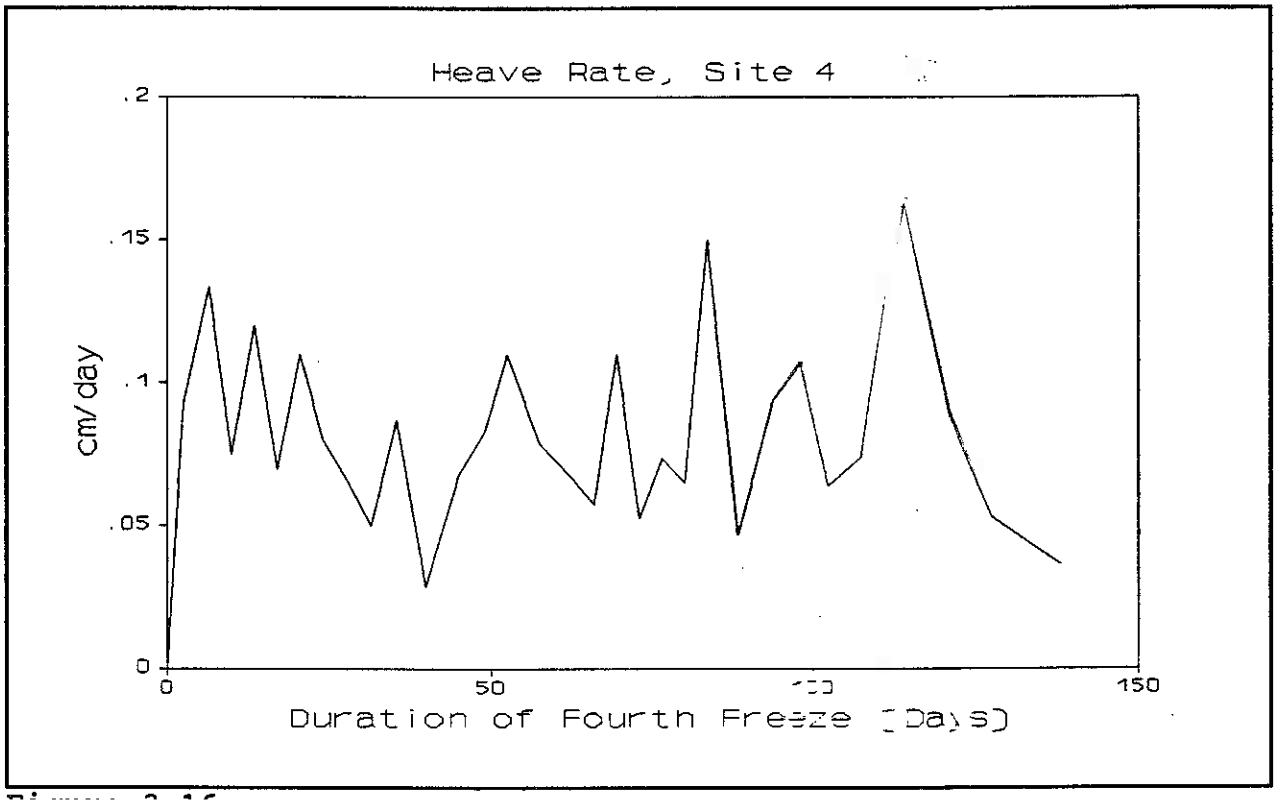
Heave Rate, Site 4
.2
.15
.1
.05
0
cm/day
0
50
150
Duration of Fourth Freeze [Days]

3.2 Soil temperatures at selected sites

Figures 3.17 to 3.19 show soil temperature data for sites 2, 3 and 4 respectively. These sites are located in the silt section near the BB transition and are located 25, 65 and 100 cm from the pipe axis.

Site 2's temperatures (Figure 3.17) are greatly affected by the pipe temperature, with the coldest temperatures being about -2.3 C at 45 cm beneath the soil surface, which corresponds to the centre of the pipe. The temperatures are warmer at all depths and times, further from the pipe axis, and the temperature gradients are smaller. These patterns are similar to those found during the third freeze cycle. Comparison with the previous freeze cycle will be made in a later report when more time has elapsed.

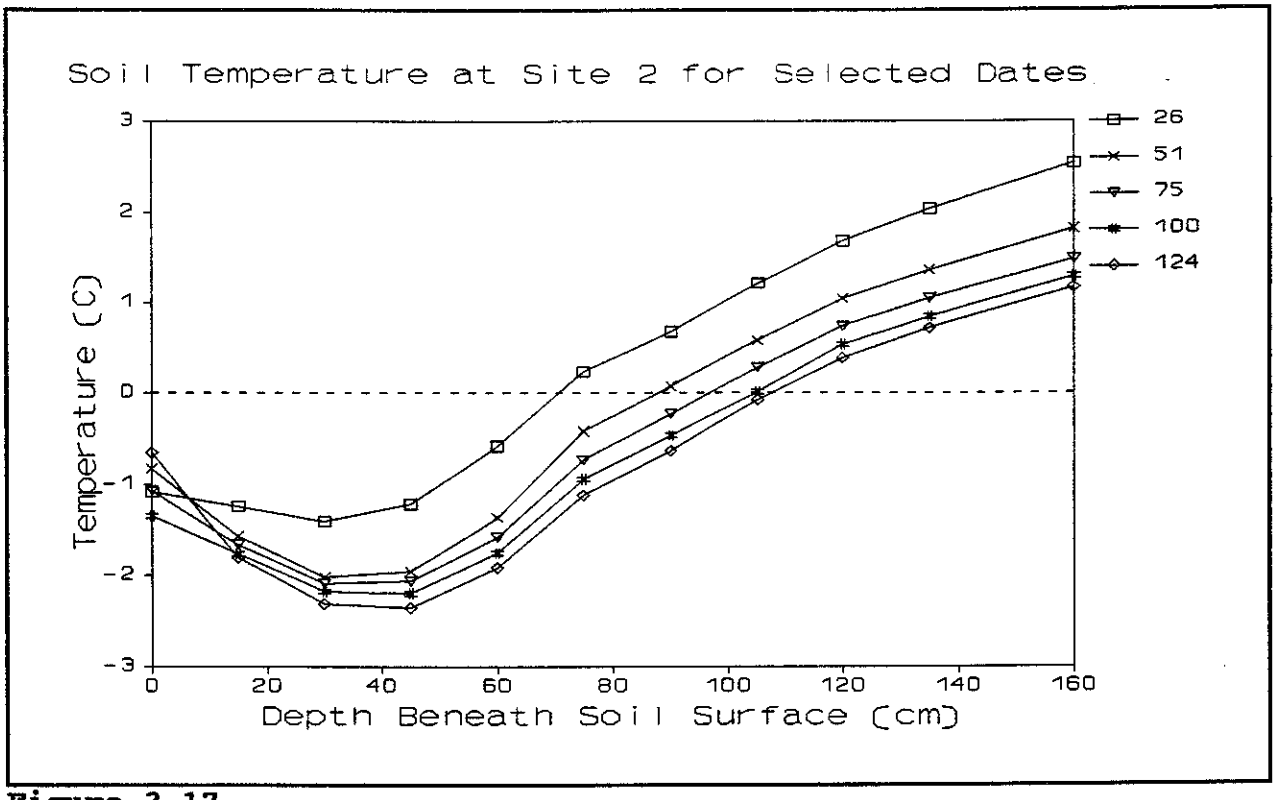
Soil Temperature at Site 2 for Selected Dates
Temperature (C)
Depth Beneath Soil Surface (cm)
26
51
75
100
124
3
2
1
0
-1
-2
-3
0
20
40
60
80
100
120
140
160

Figure 3.17

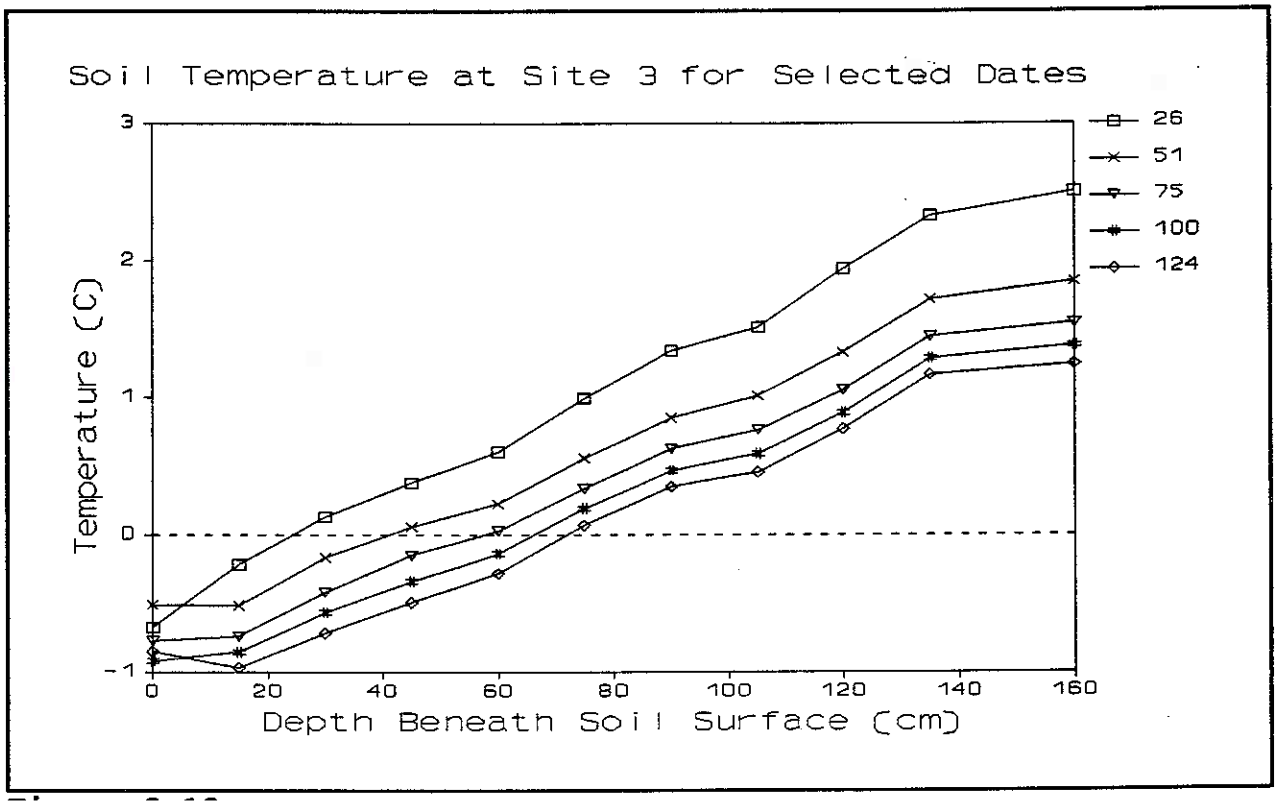
Soil Temperature at Site 3 for Selected Dates
Temperature (C)
Depth Beneath Soil Surface (cm)
26
51
75
100
124
3
2
1
0
-1
0
20
40
60
80
100
120
140
160

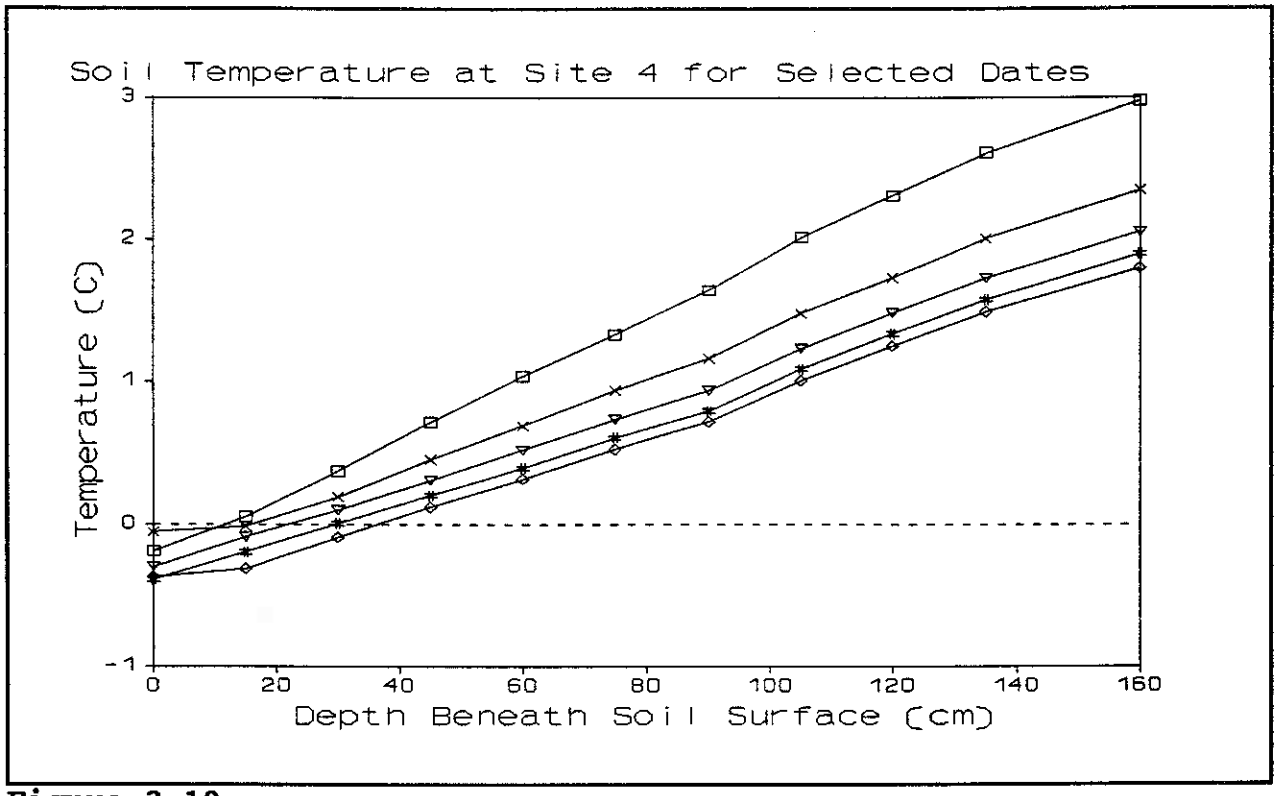

Figure 3.19

3.3 Pipe displacement

Figure 3.20 shows the pipe heave on selected dates during the fourth freeze cycle. Figure 3.21 shows the heave over time for various points along the pipe in the silt section. The heave along the pipe differ because of the constraints imposed by the pipe-frozen soil annulus which is anchored in the sand section. This effect is translated over a substantial distance and it isn't until about 6 to 7 m from the sand-silt transition that the pipe heave is more uniform (e.g. smaller variations with distance).

The amount of heave during this freeze cycle is greater than that observed during previous cycles for comparable dates and the

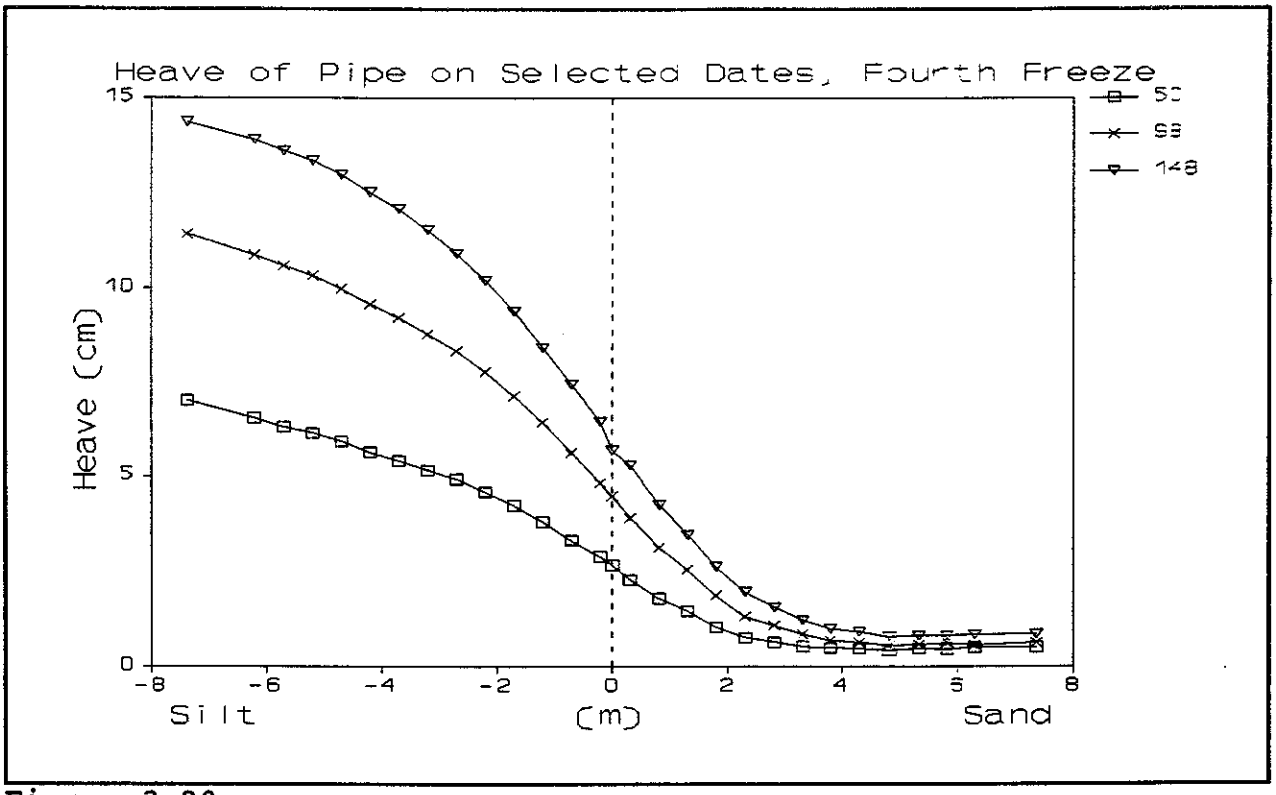
Heave of Pipe on Selected Dates, Fourth Freeze
50
98
148
Heave (cm)
15
10
5
0
-8
-6
-4
-2
0
2
4
6
8
Silt
(m)
Sand

Figure 3.20

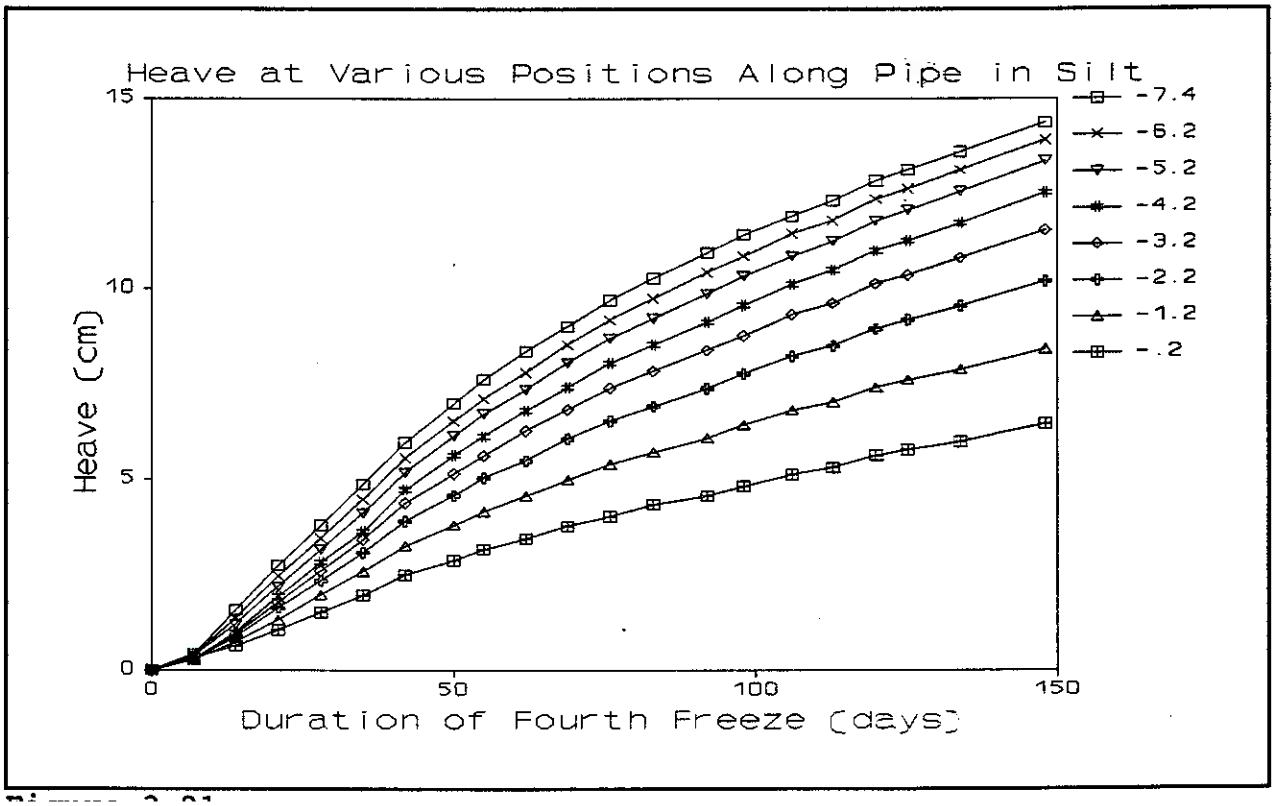
Heave at Various Positions Along Pipe in Silt
-7.4
-6.2
-5.2
-4.2
-3.2
-2.2
-1.2
-.2
Heave (cm)
15
10
5
0
0
50
100
150
Duration of Fourth Freeze (days)

same thermal conditions. This is illustrated for heave on day 99 of the three cycles:

Freeze Cycle	Heave (cm)
2 nd	9.88
3 rd	10.77
4 th	11.40

This increasing amount of heave should not, from a thermal viewpoint, occur; hence, the trend must reflect a "conditioning" of the soil. As the soil is subjected to freeze-thaw cycles, the heave susceptibility is increasing probably reflecting the development of soil micro-structure more conducive to a greater unfrozen water content and permeability. This aspect will be examined in more detailed as more data is obtained from the fourth freeze cycle.

3.4 Pipe stress

Pipe stress data for selected dates are shown in Figure 3.22. The pattern is similar to that observed in previous freeze cycles. The points of maximum stress occur about 2.3 m from the sand-silt transition in both the sand and silt sections. The stress evolution is quite rapid at first, decreasing over time.

Figure 3.23 shows the change in pipe stress over time for the strain guages having the greatest stress values (one in the sand and one in the silt at 2.3 m from the sand-silt transition). The pipe stress levels on a given date are generally greater during this cycle than on previous freeze cycles. This observation is not surprising since the pipe displacement is also greater for an equivalent date during this cycle than for

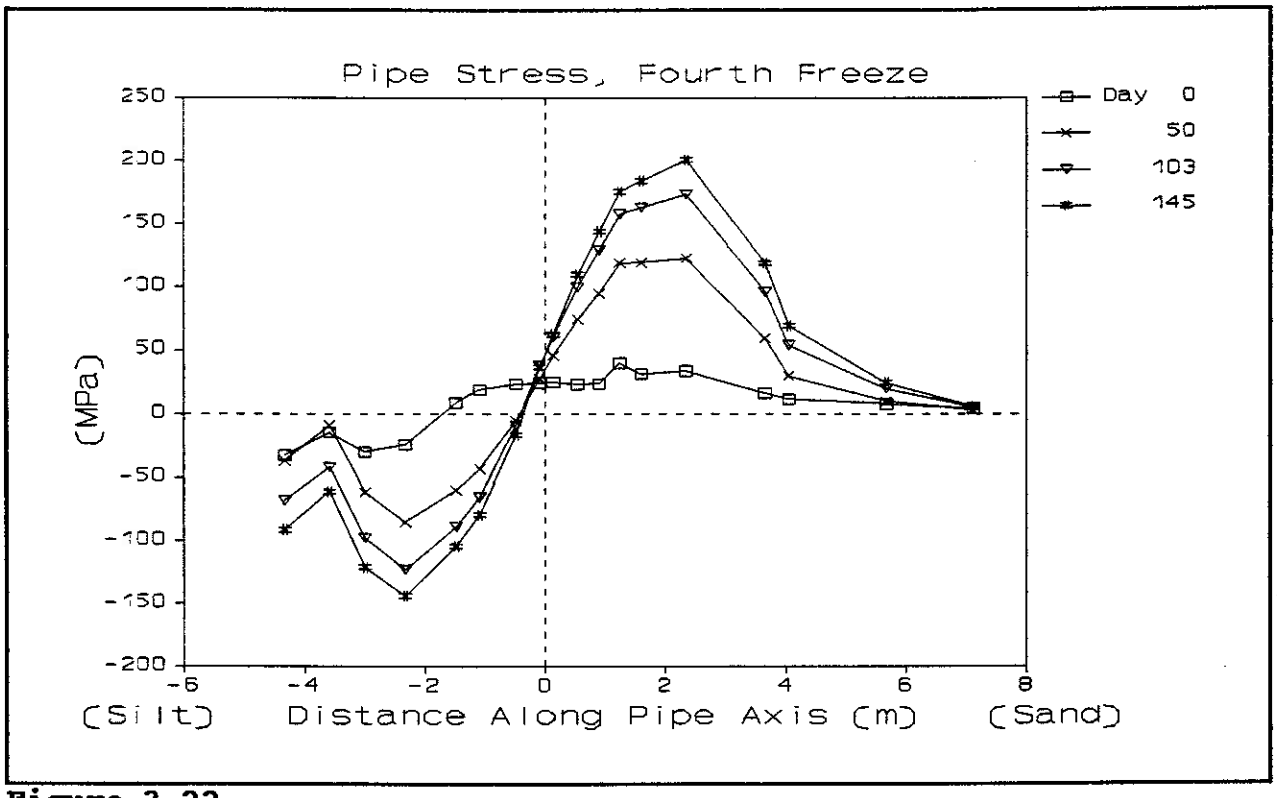
Pipe Stress, Fourth Freeze
Day 0
50
103
145
(MPa)
250
200
150
100
50
0
-50
-100
-150
-200
-6
-4
-2
0
2
4
6
8
(Silt)
Distance Along Pipe Axis (m)
(Sand)

Figure 3.22

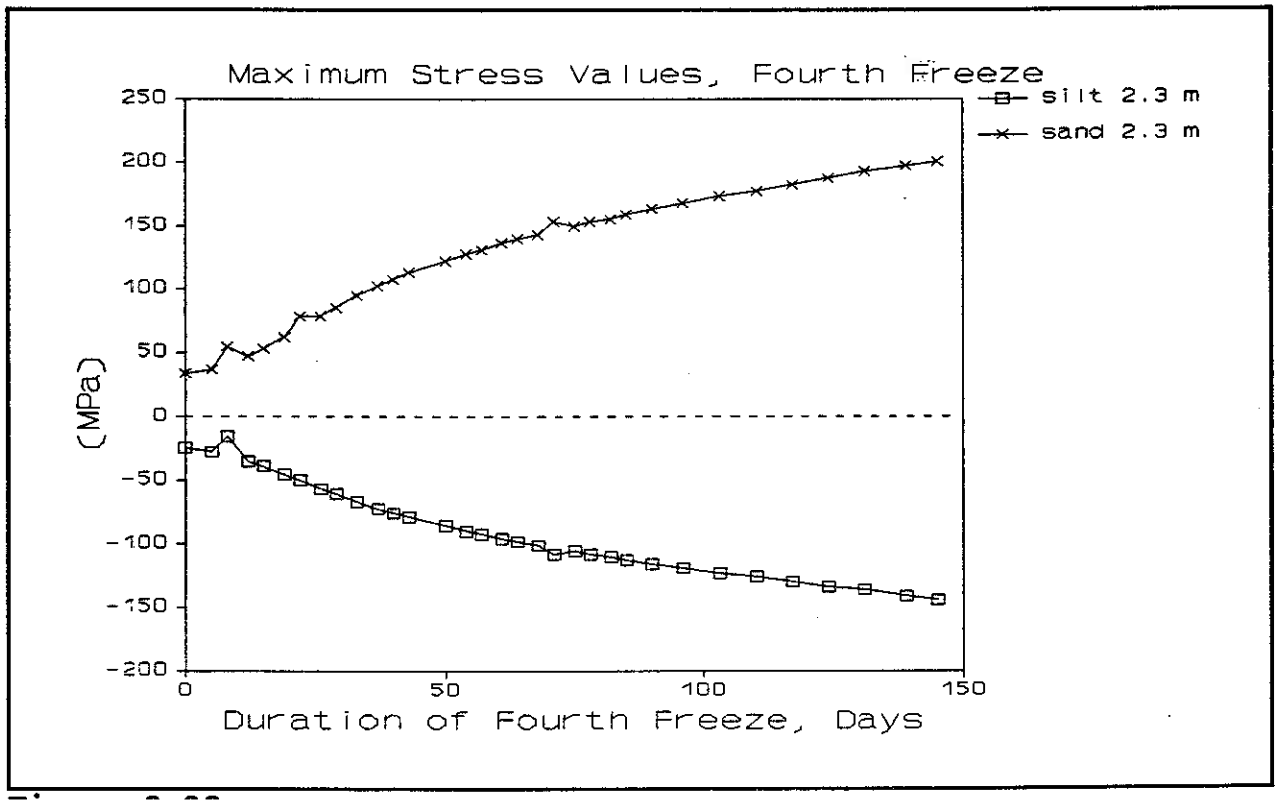
Maximum Stress Values, Fourth Freeze
silt 2.3 m
sand 2.3 m
(MPa)
250
200
150
100
50
0
-50
-100
-150
-200
0
50
100
150
Duration of Fourth Freeze, Days

3.5 Soil pressures from the Petur devices

The Petur cells were excavated and refurbished prior to the fourth freeze cycle. Many of the cells failed during the third freeze cycle because the oil-filled rubber bulbs which cover the diaphram leaked. The initial failure seems to have occurred because the rubber was not very strong and seemed to weaken when in contact with soil water for extended periods of time. A new type of rubber bulb was used which did not weaken when wet and was more robust.

Figures 3.24 and 3.25 show the change in soil pressures recorded beneath the pipe near magnet heave site 2 and near the sand-silt transition respectively. The Petur cells are labelled according to their initial position relative to the soil surface at the start of the fourth freeze cycle. These figures show that pressures rise rapidly as a cell becomes frozen in, and level off after. It is still too soon to assess whether there will be any relaxation of the surrounding material over time (eg. pressures decrease).

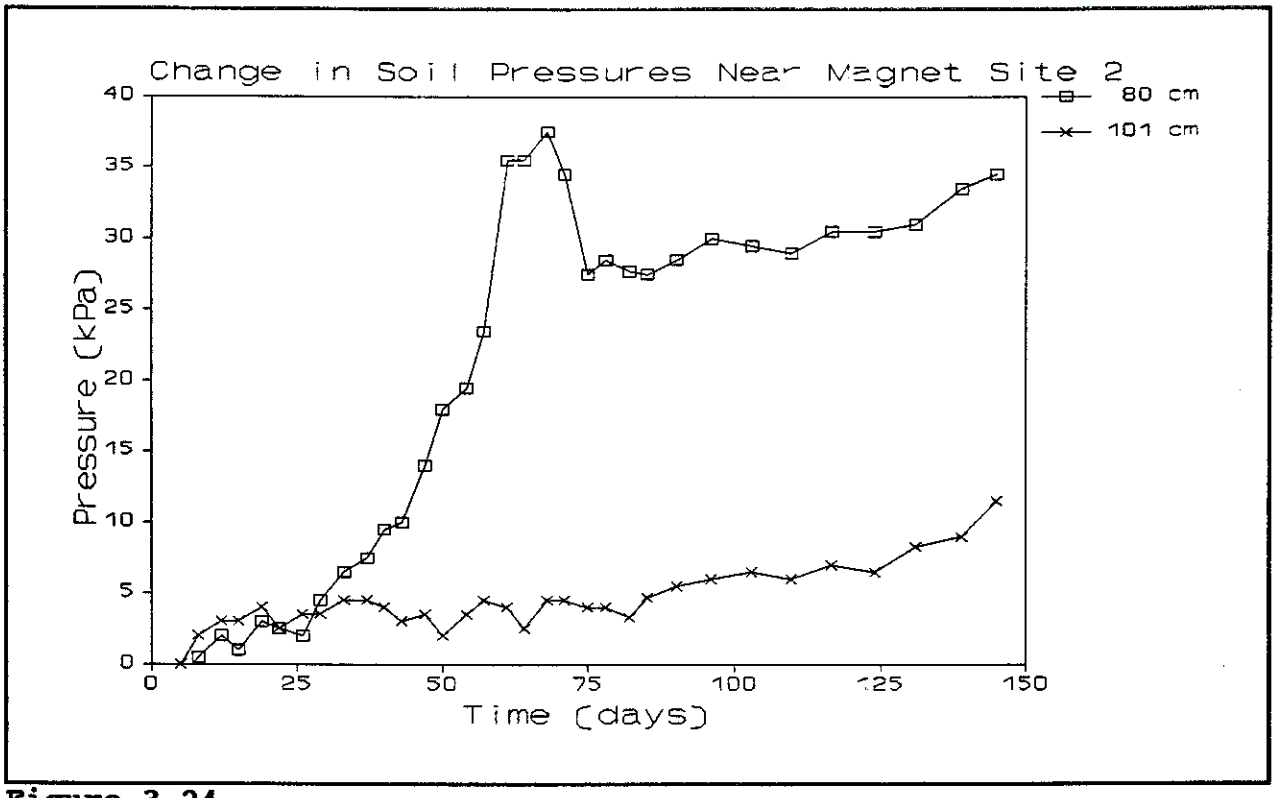

Figure 3.24

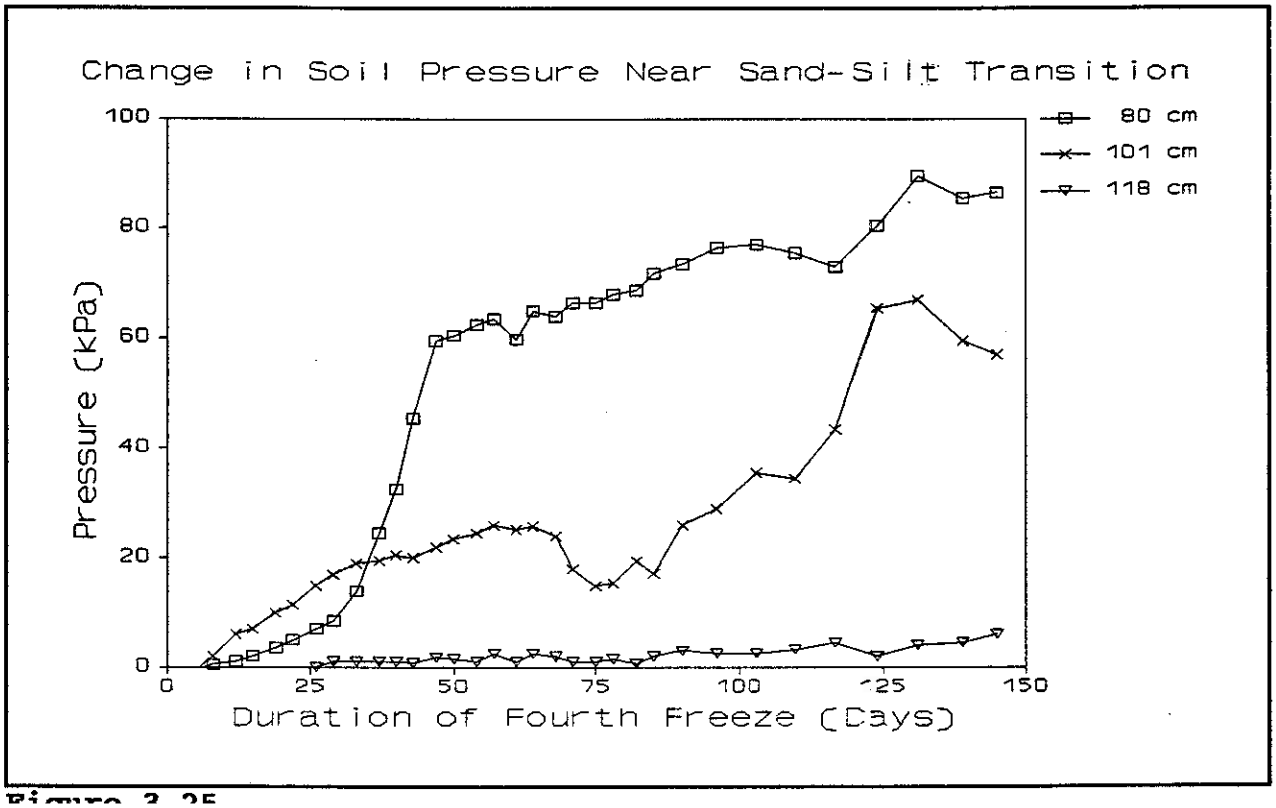

Figure 3.25

3.6 Soil pressures from Glotzl cells

The soil pressure data obtained from the Glotzl cells is similar in form and magnitude to that obtained from the Petur cells. Figure 3.26 shows the data obtained for the site located in the silt section near the BB transition. The cells are labelled according to their initial placement (prior to the first freeze cycle) beneath the pipe, hence, the 10 cm cell is about 70-75 cm beneath the soil surface.

The site shown in Figure 3.26 is fairly close to an array of Petur cells (see Figure 3.24). The form of the data is comparable although the Petur cells show a much more rapid pressure rise than is evident in the Glotzl data. This may reflect real differences which are site specific or may be due to instrumentation differences.

Figure 3.27 shows the Glotzl data for the site located beneath the pipe in the sand section near the AA transition. As in previous cycles, the pressure levels at a comparable depth are much greater in the sand than in the silt. One should also note, that the depth of frost penetration is greater in the silt, this being shown by the pressure rise (frozen in) for the 46 cm cell on about day 40.

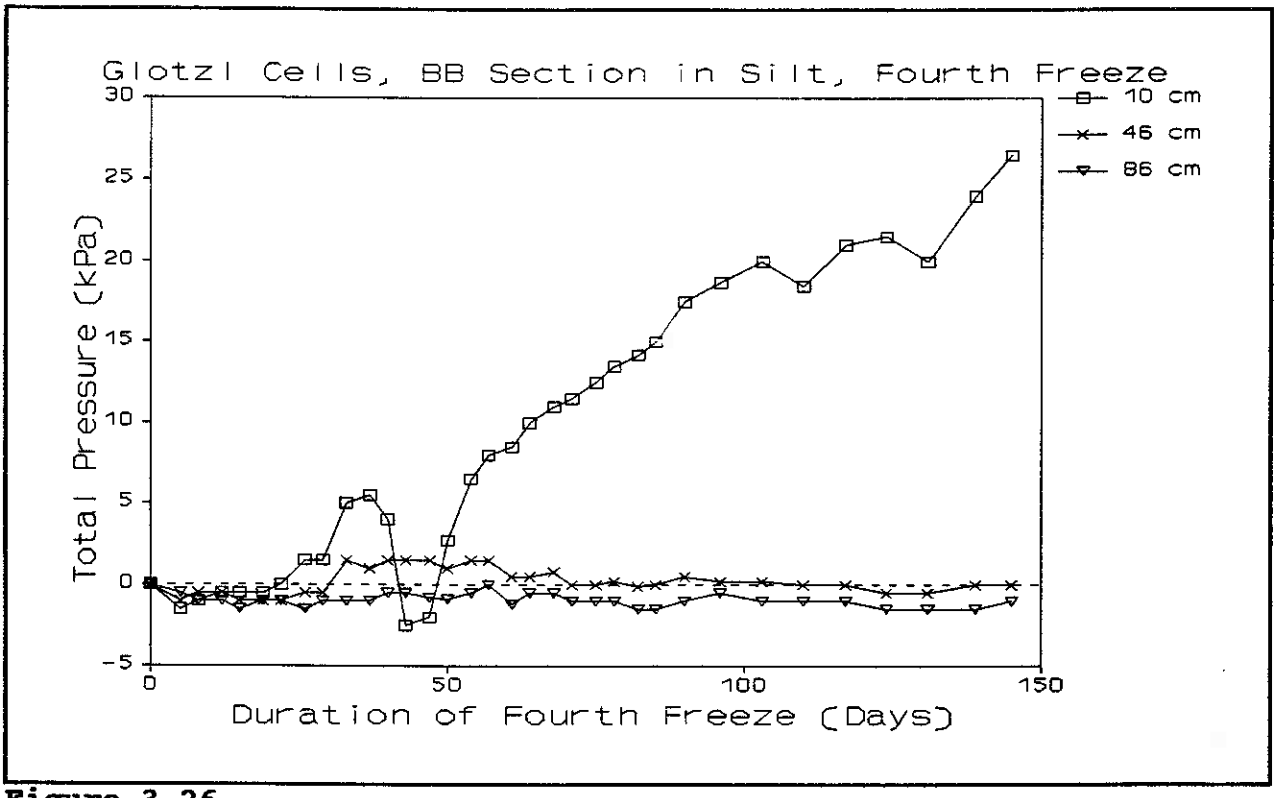
Glotzl Cells, BB Section in Silt, Fourth Freeze
10 cm
46 cm
86 cm
Total Pressure (kPa)
30
25
20
15
10
5
0
-5
0
50
100
150
Duration of Fourth Freeze (Days)

Figure 3.26

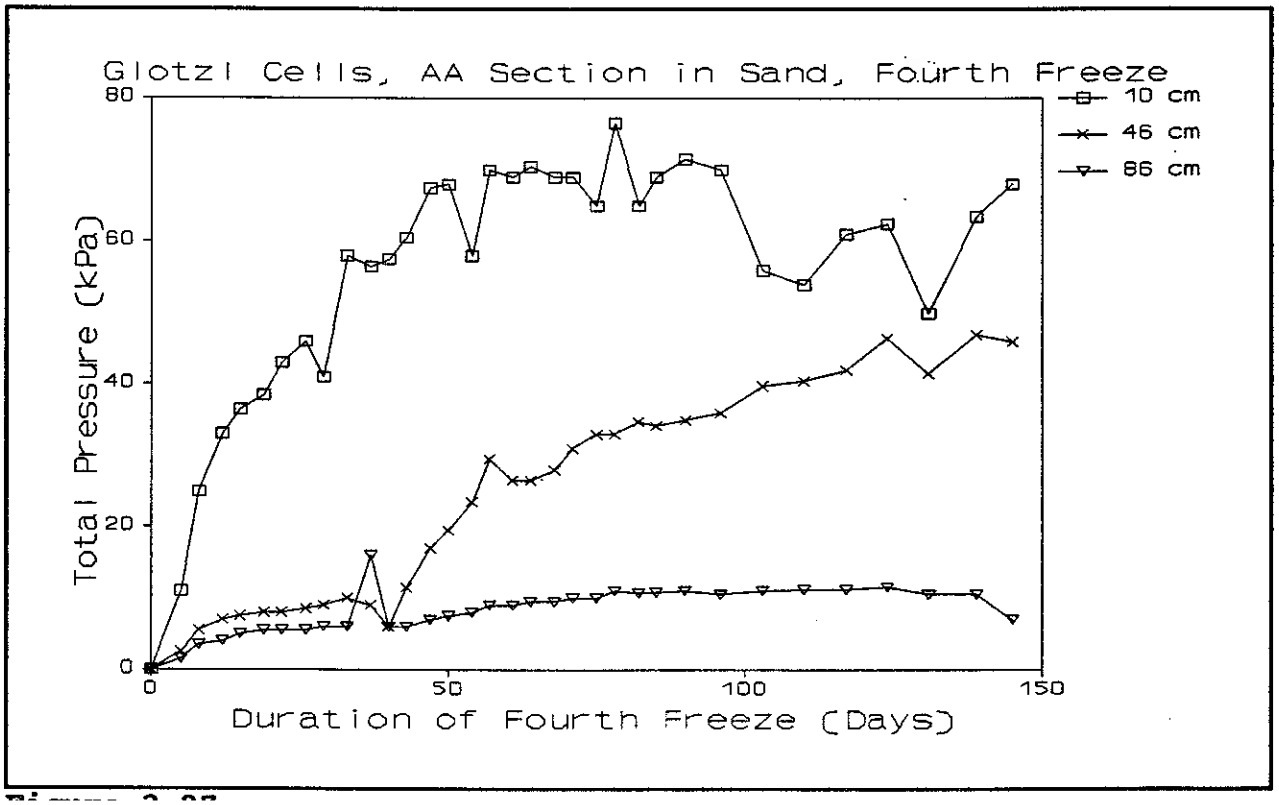
Glotzl Cells, AA Section in Sand, Fourth Freeze
10 cm
46 cm
86 cm
Total Pressure (kPa)
80
60
40
20
0
0
50
100
150
Duration of Fourth Freeze (Days)

4. A mathematical model for calculating stress and deformation fields in soils during freezing

The volume expansion of freezing soil is caused by the fact that water in soil is changed into ice and the moisture content increases by the moisture migrating from unfrozen to frozen soil. Thus, the calculation of stresses and deformations in soil must deal with the coupled heat and moisture transfer under variable stresses. During the past two decades, many numerical models for simulating the heat and moisture transfer during frost heaving have been proposed. However, most of these models do not consider the effects of external loading; they assume that the soil is under zero load and ice at atmospheric pressure. Blanchard and Fremond (1985) were the first ones to propose the model for coupling the heat, moisture and stress fields, on the basis of the principle of conservation of energy, mass and momentum. They have up to now applied this model successfully for simulating heat and moisture transfer around the pipeline, but no information on the stress field was given. In our model (Shen and Ladanyi, 1987), another relatively simple way for coupling together the heat, moisture and stress effects is proposed. The main differences between the two models are that we are using the Clapeyron equation (1) to describe the effect of the stress field on the heat and moisture transfer on the basis of some assumptions about the ice pressure distribution in the freezing fringe; (2) the Prandtl-Reuss law to determine the creep strains due to the stress field, and (3) the incremental initial

strain method for defining the stress distribution produced by the volumetric strain of freezing soil caused by the phase change of water and moisture transfer. This model is shown to be quite suitable for predicting the stress and deformation fields in freezing soil. From the practical viewpoint, the prediction of stress and deformation distribution during frost heaving are of a great importance for prediction of stability of structures in cold regions.

For the heat transfer, if the convective heat transfer by thermal vapour is negligible, the heat transport equation may be written as:

$$C \cdot \frac{\partial T}{\partial \tau} = \nabla \cdot (\lambda \nabla T) + L \rho_i \frac{\partial \theta_i}{\partial \tau} \qquad (1)$$

where C, is the heat capacity of the soil (J m^{-3} C^{-1}); λ, is the thermal conductivity of the soil (W m^{-1} C^{-1}); T, is temperature (C); L is the latent heat of fusion (J kg^{-1}); and, τ, is time (s).

For the moisture transfer, if the mass transport of water in frozen soil is assumed to take place only by liquid flow, the equation can be written as:

$$\frac{\partial}{\partial \tau}\left[\theta_l + \frac{\rho_i \theta_i}{\rho_l}\right] = \nabla (K \cdot \nabla P_l) \qquad (2)$$

where ρ_l and ρ_i are the densities of liquid water and ice (kg m^{-3}); θ_l and θ_i are the volumetric fractions of liquid water and ice; k is the hydraulic conductivity (m^2 s^{-1} Pa^{-1}) and P_l is the liquid water pressure (Pa).

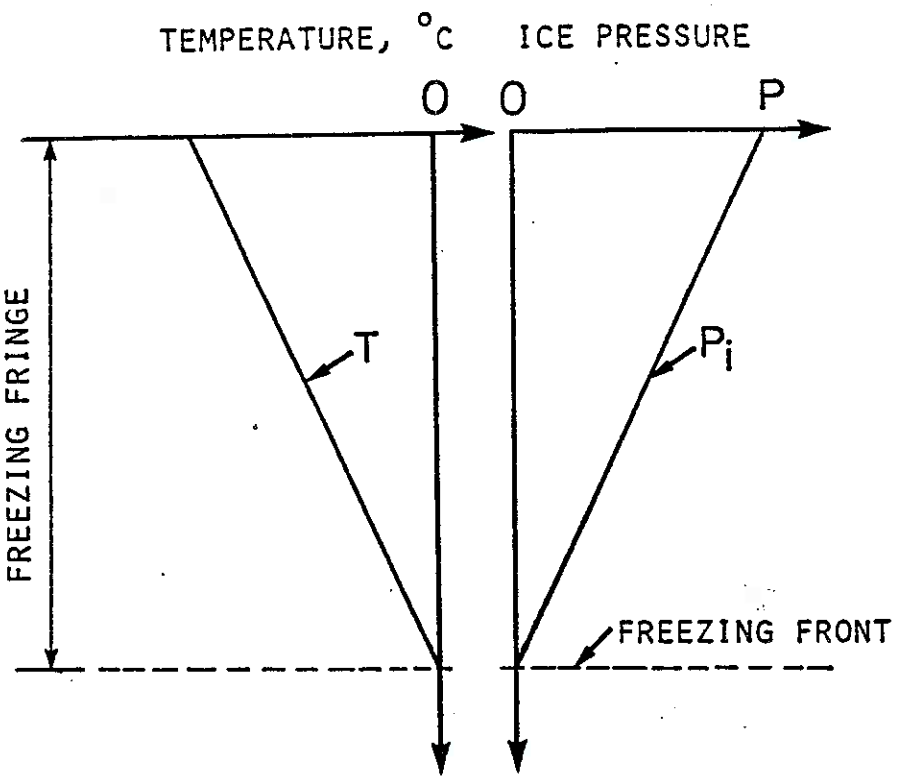

Fig.4.1. Idealized distribution of temperature and ice pressure within the freezing fringe, adopted in the calculation.

The pressure of liquid water P_l in frozen soil can be described by the Clapeyron equation:

$$\frac{P_L}{\rho_L} - \frac{P_i}{\rho_i} = L \cdot \ln \frac{T_k}{T_0} \tag{3}$$

In order to use this equation, we have assumed that the ice pressure P_i at the freezing front is zero, and that at the coldest side of the freezing fringe it is equal to the local mean pressure (Figure 4.1). The criterion for frost heaving is that the ice content exceeds a critical value equal to 85% of the soil porosity, regardless of the unfrozen water content.

Once the ice pressure P_i is defined, substituting (3) and (2) into (1), and rearranging gives:

$$\bar{C} \frac{\partial T}{\partial \tau} = \nabla(\bar{\lambda} \nabla T) + \rho_L \cdot L \cdot \nabla(K \cdot \nabla P_L) \tag{4a}$$

with

$$\bar{C} = C + L \cdot \rho_L \cdot \frac{\partial \theta_L}{\partial T} \tag{4b}$$

$$\bar{\lambda} = \lambda + \frac{k \rho_L^2 L^2}{T_K} \tag{4c}$$

In fact, the effect of stress on heat transfer is very small and may be neglected. Equation 4 can be rewritten as:

$$\bar{C} \frac{\partial T}{\partial \tau} = \nabla(\bar{\lambda} \cdot \nabla \cdot T) \tag{5}$$

The basic equations for heat and moisture transfer in the model are equations (5), (2) and (3). In these equations, the relationship between the unfrozen water content and temperature

must be determined experimentally.

If the volume of soil particles is assumed to remain constant during the freezing process, the volumetric expansion strain ϵ^v caused by the moisture transfer and by the pore water transformation into ice, can be given by:

$$\epsilon^v = 0.09(\theta_0 + \Delta\theta - \theta_L) + \Delta\theta + (\theta_0 - n) \tag{6}$$

where θ_0, is the initial water content ($m^3\ m^{-3}$); $\Delta\theta$ is the increment of water content ($m^3\ m^{-3}$); and n, is the porosity of the soil.

Because the soil is considered to be isotropic, the normal expansion strain in each direction is equal, and the shear strain due to the expansion is zero, giving:

$$\epsilon_{ij} = \frac{1}{3} \cdot \delta_{ij} \cdot \epsilon^v \tag{7}$$

where δ_{ij} is Kronecker delta.

Under external loading, the stress-strain relationship of frozen soil is given by the following incremental form:

$$d\{\sigma\} = [D](d\{\epsilon\} - d\{\epsilon^c\} - d\{\epsilon^v\}) \tag{8}$$

where $d\{\sigma\}$ is the stress increment vector; [D], is the matrix of elastic constants related to the temperature of frozen soil; $d\{\epsilon\}$, $d\{\epsilon^c\}$, $d\{\epsilon^v\}$ are strain increment vectors, creep increment vector and expansion strain increment vector, respectively.

According to the Prandtl-Reuss law, the creep strain

increment vector may be written as:

$$d\{\epsilon^c\} = d\bar{\epsilon}^c \frac{\partial \bar{\sigma}}{\partial \{\sigma\}} \tag{9}$$

where $\bar{\epsilon}^c$ and $\bar{\sigma}$ are von Mises equivalent creep strain and equivalent stress. In multiaxial states of stress, the empirical power creep law adopted in the uniaxial case can be generalized as follows (Ladanyi, 1983):

$$\bar{\epsilon}^c = \left[\frac{\bar{\sigma}}{\sigma_{cT}}\right]^n \left[\frac{\dot{\epsilon}^c_T}{b}\right]^b \tag{10a}$$

with

$$\sigma_{cT} = \sigma_{co}\left[1 + \frac{T}{T_r}\right]^{\omega} \tag{10b}$$

where n, b, ω are experimental coefficients, and $\dot{\epsilon}^c$, σ_{co} and T_r = -1 °C, are reference values of strain rate, stress and temperature.

From equations (6), (9) and (10) the equivalent nodal forces increment vector $\Delta\{R\}$ due to creep and volumetric expansion in soil, can be written as:

$$\Delta\{R\} = \iiint [B]^T [D] \Delta\{\epsilon^v\} dV + \iiint [B]^T [D] \cdot b \cdot \left[\frac{\bar{\sigma}}{\sigma_{cT}}\right]^n \left[\frac{\dot{\epsilon}^c}{b}\right]^b \tau^{b-1} \frac{\partial \bar{\sigma}}{\partial \{\sigma\}} \cdot \Delta\tau \cdot dV \tag{11}$$

The above equations constitute the system of equations for calculating stress and deformation increments in each time step by the finite element method.

This model was shown to simulate successfully unidirectional

freezing of a cylindrical sample (Penner, 1986). The simulation furnished the complete stress field, and the effect of external loading on the amount of frost heaving. We are presently extending this model in order to be able to calculate the stress and deformation fields around a chilled pipeline buried in a freezing soil.

References

Blanchard, D. and M. Fremond. 1985. Soils frost heaving and thaw settlement, Proceedings of the 4th International Symposium on Ground Freezing, pp. 209-216.

Geotechnical Science Laboratories, 1982. Feasibility studies for stresses in a pipeline buried in freezing soil. Report to Energy, Mines and Resources, Canada, Earth Physics Branch. 36 pp.

Geotechnical Science Laboratories, 1983. Investigation of soil freezing in association with a buried chilled pipeline in a large-scale test facility, Phase 2. 41 pp.

Geotechnical Science Laboratories, 1984a. Analysis of stresses developed in pipelines buried in freezing ground. Report to Energy, Mines and Resources, Canada, Earth Physics Branch, 59 pp.

Geotechnical Science Laboratories, 1984b. Experimentation sur le gel d'un sol et d'une canalisation enterree et refroidie dans une installation d'essai de grandes dimensions 3e phase. Rapport pour le Ministere de l'Energie, Mines et Ressources, Direction de la Physique du Globe. 73 pp.

Geotechnical Science Laboratories, 1985. Analyses of stresses developed in pipelines buried in freezing ground. Final report for Earth Physics Branch, Energy, Mines and Resources, 39pp.

Geotechnical Science Laboratories, 1988. The Third Freeze Cycle of the Canada-France Ground Freezing Experiment. Final report for Earth Physics Branch, Energy, Mines and Resources

Konrad, J.-M. and N.R.Morgenstern. 1981. The segregation potential of a freezing soil. Canadian Geotechnical Journal, 18: 482-491.

Ladanyi, B. 1983. Shallow foundations on frozen soil: Creep settlement, Journal Geotechnical Engineering, ASCE, Vol. 109, No. 11, pp. 1434-1448.

Miller, R.D. 1972. Freezing and heaving of saturated and unsaturated soils, Highway Research Record, Vol. 393, pp. 1-11.

Penner, E. 1986. Aspects of ice lens growth in soils, Cold

Regions Science and Technology, Vol. 13, No. 1, pp. 91-100.

Shen, M. and B. Ladanyi 1987. Modelling of coupled heat, moisture and stress field in freezing soil, Cold Regions Science and Technology, Vol. 14, No. 3, pp. 237-246.

Shen, M. and B. Ladanyi, 1988. Calculation of stress field in soil during freezing. Procedings of the 5th International Symposium on Ground Freezing.

Smith, M.W. and D.E. Patterson (submitted for publication)